

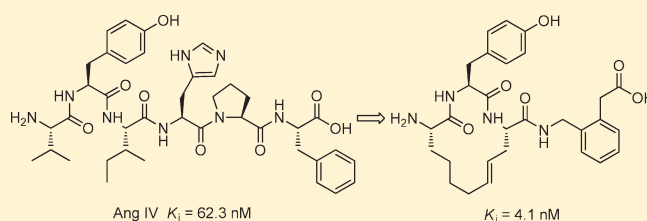
Potent Macrocyclic Inhibitors of Insulin-Regulated Aminopeptidase (IRAP) by Olefin Ring-Closing Metathesis

Hanna Andersson,[†] Heidi Demaegdt,[‡] Anders Johnsson,[†] Georges Vauquelin,[‡] Gunnar Lindeberg,[†] Mathias Hallberg,[§] Máté Erdélyi,^{||,⊥} Anders Karlén,[†] and Anders Hallberg^{*,†}[†]Department of Medicinal Chemistry, Uppsala University, Box 574, SE-751 23 Uppsala, Sweden[‡]Department of Molecular and Biochemical Pharmacology, Vrije Universiteit Brussel, Pleinlaan 2, 1050 Brussels, Belgium[§]Department of Pharmaceutical Biosciences, Uppsala University, Box 591, SE-751 24 Uppsala, Sweden^{||}Department of Chemistry, University of Gothenburg, SE-412 96 Gothenburg, Sweden[⊥]Swedish NMR Centre, University of Gothenburg, Box 465, SE-405 30 Gothenburg, Sweden

S Supporting Information

ABSTRACT: Macrocyclic analogues of angiotensin IV (Ang IV, Val¹-Tyr²-Ile³-His⁴-Pro⁵-Phe⁶) targeting the insulin-regulated aminopeptidase (IRAP) have been designed, synthesized, and evaluated biologically. Replacement of His⁴-Pro⁵-Phe⁶ by a 2-(aminomethyl)phenylacetic acid (AMPAA) moiety and of Val¹ and Ile³ by amino acids bearing olefinic side chains followed by macrocyclization provided potent IRAP inhibitors.

The impact of the ring size and the type (saturated versus unsaturated), configuration, and position of the carbon–carbon bridge was assessed. The ring size generally affects the potency more than the carbon–carbon bond characteristics. Replacing Tyr² by β³hTyr or Phe is accepted, while N-methylation of Tyr² is deleterious for activity. Removal of the carboxyl group in the C-terminal slightly reduced the potency. Inhibitors **7** ($K_i = 4.1$ nM) and **19** ($K_i = 1.8$ nM), both encompassing 14-membered ring systems connected to AMPAA, are 10-fold more potent than Ang IV and are also more selective over aminopeptidase N (AP-N). Both compounds displayed high stability against proteolysis by metallopeptidases.



INTRODUCTION

Angiotensin IV (Ang IV, Val¹-Tyr²-Ile³-His⁴-Pro⁵-Phe⁶), one of the bioactive peptides of the renin–angiotensin system (RAS), is known to play an important role in cognitive processes.^{1–18} The hexapeptide improves memory and learning, as has been demonstrated in a large number of animal studies over the past 20 years (reviewed by Wright et al.¹⁹). Ang IV binds with high affinity to the insulin-regulated aminopeptidase (IRAP, EC 3.4.11.3),²⁰ an enzyme localized in areas of the brain associated with memory and learning.^{21–23} IRAP, frequently colocalized with the insulin-responsive glucose transporter GLUT4,²⁴ is a type II transmembrane protein that belongs to the same family of aminopeptidases as aminopeptidase N (AP-N).²⁵ In recent years, IRAP has emerged as a promising new target for drug intervention, and selective inhibition of this enzyme might provide a new approach in the treatment of memory dysfunction.^{26–28} Furthermore, clinical studies of the cholinesterase inhibitors and NMDA antagonists presently used in the treatment of Alzheimer's disease have been mostly disappointing.^{29–32} Thus, there is a strong demand for efficient agents, conceivably relying on alternative mechanisms for the treatment of the cognitive decline associated not only with Alzheimer's disease, brain trauma, and cerebral ischemia but also with other age-related neurological diseases. New avenues have

to be explored to enable the development of significantly improved enhancers of cognitive function.

The first SAR studies on Ang IV analogues targeting the binding site of Ang IV were reported from the research groups of Wright and Harding.^{33–35} Their continuous work focusing on developing more druglike Ang IV analogues have led to the discovery of *N*-hexanoyl-Tyr-Ile-*N'*-(5-carbamoylpentyl)amide (PNB-0408), which is a blood–brain barrier permeable compound exhibiting cognitive-enhancing activity.^{19,28,36,37} The activity profiles of this modified tripeptide and related analogues in several animal models of dementia are now being established.^{28,36} From a β-homoamino acid scan of Ang IV followed by replacement of His⁴ or His⁴-Pro⁵ by conformationally constrained residues, Lukaszuk et al. have developed a number of potent, selective and stable five- and six-residue analogues of Ang IV,^{38,39} e.g., **1** (AL-40, Figure 1).³⁸ In 2008, a new druglike series of chromene-based nonpeptidic IRAP inhibitors, e.g., **2** (HFI-437, Figure 1), was identified by Albiston et al. by utilizing a combination of homology modeling of the catalytic domain of IRAP and in silico screening methodologies.^{40,41} The performance

Received: January 12, 2011

Published: April 08, 2011

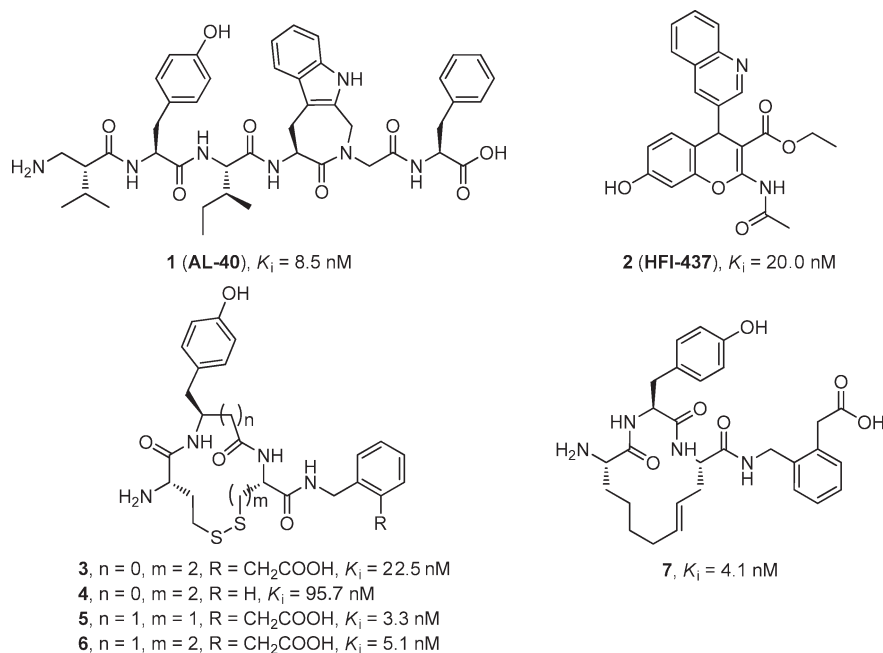


Figure 1. Macrocyclic IRAP inhibitor 7 together with recently identified peptidomimetic (1^{38} and $3-6^{45}$) and nonpeptidic (2^{40}) inhibitors.

in both spatial working and recognition memory paradigms was improved after administering one of the inhibitors to the lateral ventricles.⁴⁰ This observation strongly supports the hypothesis that IRAP provides a relevant enzyme target in the search for new enhancers of cognition. Recently a study involving molecular docking and site-directed mutagenesis was published. It was concluded that Phe⁵⁴⁴ in IRAP plays an essential role in defining the interaction of 2 and similar IRAP inhibitors with the catalytic site of the protease.⁴¹

In the search for druglike Ang IV peptidomimetics as efficient IRAP inhibitors we initiated a program employing an alternative, substrate-based strategy starting with introduction of steric constraints.^{42–45} Macrocyclization of linear molecules offers many significant advantages. It reduces the accessible conformational space and frequently affords ligands with high target affinity and better metabolic stability, membrane permeability, and selectivity.⁴⁶ We recently reported that formation of 11- to 13-membered rings by disulfide cyclizations of Ang IV in both the N- and C-terminal ends and subsequent structural modifications relying on conformational analyses provided IRAP inhibitors, exemplified by 3–6 (Figure 1).⁴⁵

We here report that replacement of the chemically and metabolically labile disulfide bonds by carbon–carbon bonds via macrocyclization employing the olefin ring-closing metathesis reaction (RCM) provided potent IRAP inhibitors (e.g., 7, Figure 1).^{47–51} The present transformation is well recognized for producing analogues with altered metabolic stability, biological activity, and conformational properties.^{52–56}

RESULTS AND DISCUSSION

Chemistry. The compounds presented in Table 1 (7–10 and 17–26) were prepared by manual SPPS using the 9-fluorenylmethoxycarbonyl (Fmoc) protection strategy,⁵⁷ followed by side chain to side chain cyclization between residues 1 and 3 by RCM,^{47,48,50,51} as outlined in Schemes 1–3. Two different

strategies were adopted: cyclization of the Fmoc protected linear sequence attached to the solid phase (Schemes 1 and 2) or in solution (Scheme 3).

The initial strategy was to perform RCM with the linear sequence attached to the resin.⁵⁸ The stability of the polymer-bound linkers and reagents is one of the major concerns when applying microwave heating in solid-phase synthesis. The Wang and 4-(4-formyl-3-methoxyphenoxy)butyrylaminoethyl (FMPB AM) resins have been shown to withstand a variety of conditions, including high temperatures,⁵⁹ and were thus chosen for the synthesis of the desired compounds. The Grubbs second generation catalyst (GII) and Hoveyda–Grubbs second generation catalyst (HGII) were evaluated, using 1,2-dichloroethane (DCE) as solvent and microwave heating at a variety of temperatures for up to 1 h. From these results the cyclization was performed in preparative scale using HGII (0.15 equiv) at 150 °C for 5 min and repeated once after the second addition of catalyst. The resins were treated with DMSO (30 equiv) in CH_2Cl_2 overnight for scavenging of ruthenium contaminants before deprotection and cleavage.^{60,61} Complex mixtures of poorly separable compounds were obtained, and only one compound (7) could be purified at a sufficient amount. In addition to isomerization before ring closure, leading to ring-contracted products, double bond migration after ring closure was observed. Analogue 7 is a result of a one-step shift of the double bond position toward the backbone. Some product mixtures were subjected to catalytic hydrogenation to obtain the corresponding saturated compounds. To allow faster evaluation and better control over the cyclization step, a solution-phase approach was adopted. The conditions were re-evaluated, and the reactions were performed in the presence and absence of benzoquinones. Electron-deficient benzoquinones such as 2,6-dichloro-1,4-benzoquinone and tetrafluoro-1,4-benzoquinone have been found to prevent undesirable isomerization during RCM.⁶² Here, both 2,6-dichloro-1,4-benzoquinone and 1,4-benzoquinone (BQ) were efficient in suppressing double-bond migration and the formation of ring-contracted products, while

Table 1. Stability and Inhibition Activities of Ang IV and Analogues 7–10 and 17–26^d

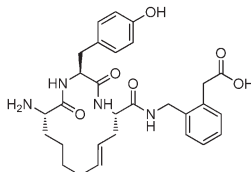
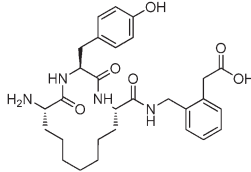
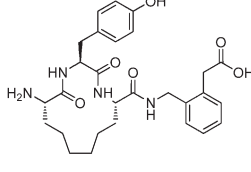
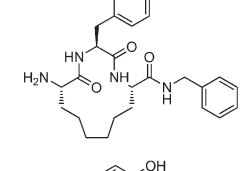
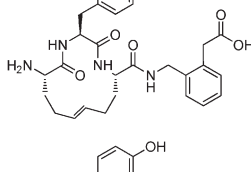
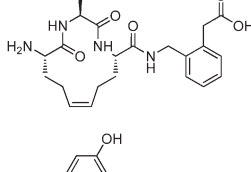
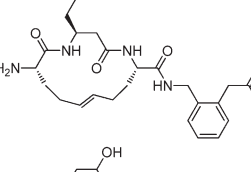
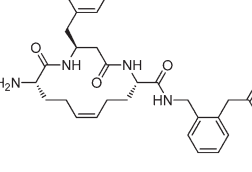
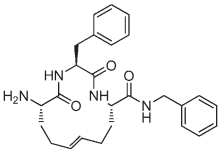
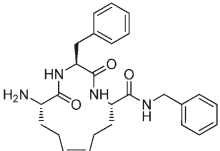
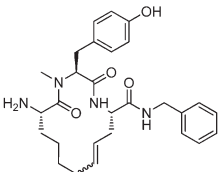
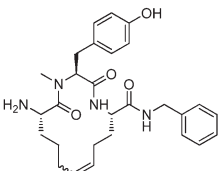
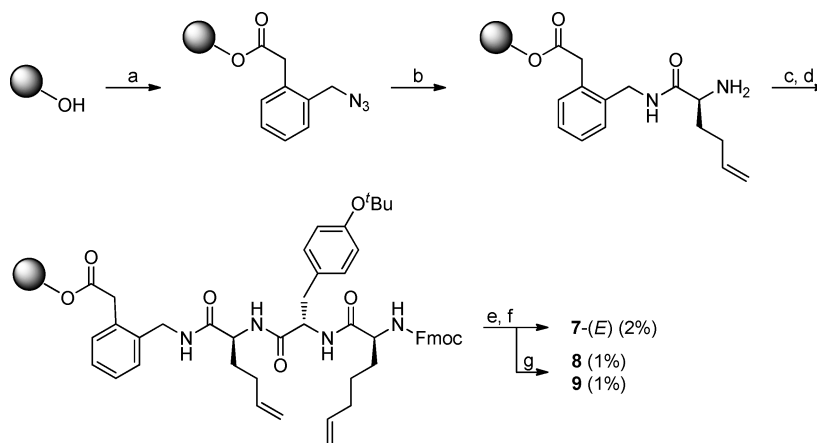
No	Sequence/Structure	Binding affinity $K_i \pm SD$ (nM) ^a		Enzyme $K_i \pm SD$ (nM)	
		Chelators	No chelators	IRAP ^b	AP-N ^c
Ang IV	Val-Tyr-Ile-His-Pro-Phe	9.3 ± 2.9	1139 ± 1329	62.4 ± 17.5	841 ± 38
7		46.8 ± 35.3	133 ± 14	4.1 ± 0.2	4955 ± 490
8		12.5 ± 0.5	517 ± 119	25.0 ± 4.0	12 000 ± 3500
9		28.9 ± 0.8	631 ± 448	64.2 ± 9.2	3283 ± 83
10				193 ± 50	8345 ± 239
17		36.8 ± 2.3	450 ± 15	50.0 ± 5.5	1074 ± 206
18		24.8 ± 1.9	568 ± 12	41.1 ± 9.7	5413 ± 1656
19		9.8 ± 0.6	74.2 ± 6.6	1.8 ± 0.1	240 ± 28
20		24.5 ± 2.9	468 ± 11	30.4 ± 0.8	1299 ± 260

Table 1. Continued

No	Sequence/Structure	Binding affinity $K_i \pm SD$ (nM) ^a		Enzyme $K_i \pm SD$ (nM)	
		Chelators	No chelators	IRAP ^b	AP-N ^c
21		719 ± 217	3520 ± 987	697 ± 20	1571 ± 163
22		287 ± 50	3468 ± 2126	351 ± 51	12 000 ± 1400
23-(<i>E</i>)				5845 ± 1080	N.M.
24-(<i>Z</i>)				4011 ± 1513	N.M.
25-(<i>E</i>)				12 000 ± 5400	N.M.
26-(<i>Z</i>)				10 800 ± 5000	N.M.

^a [³H]AL-11 competition binding in CHO-K1 cell membranes.⁷⁶ ^b Evaluated in an enzyme assay comprising recombinant human IRAP transiently transfected in HEK293 cells. ^c Evaluated in an enzyme assay comprising recombinant human AP-N transiently transfected in HEK293 cells. ^d SD, standard deviation. N.M., not measurable (>100 μM).

Scheme 1. Synthesis of 7–9 Using Wang Resin^a

^a Reagents and conditions: (a) (i) 2-(azidomethyl)phenylacetic acid, DIC, DMAP, DMF/CH₂Cl₂ (1:9), 44 °C, 3 h, (ii) acetic anhydride (5.0 equiv), pyridine (1.0 equiv), DMF, 0.5 h; (b) (i) Fmoc-Hag-OH, DIC, HOBT, CH₂Cl₂, (ii) PBu₃, room temp, on, (iii) 20% piperidine/DMF; (c) (i) Fmoc-Tyr(^tBu)-OH, HATU, DIEA, DMF, room temp, 2 h, (ii) 20% piperidine/DMF; (d) (2*S*)-Fmoc-2-amino-6-heptenoic acid, HATU, DIEA, DMF, room temp, 2 h; (e) (i) HGII, DCE, microwave, 140 °C, 5 min, (ii) HGII, DCE, microwave, 140 °C, 5 min, (iii) DMSO, CH₂Cl₂, room temp, on, (iv) 20% piperidine/DMF; (f) trifluoroacetic acid (TFA)/triethylsilane (TES)/H₂O (90:5:5), room temp, 2 h; (g) H₂, Pd/C, EtOH, room temp, 4 h.

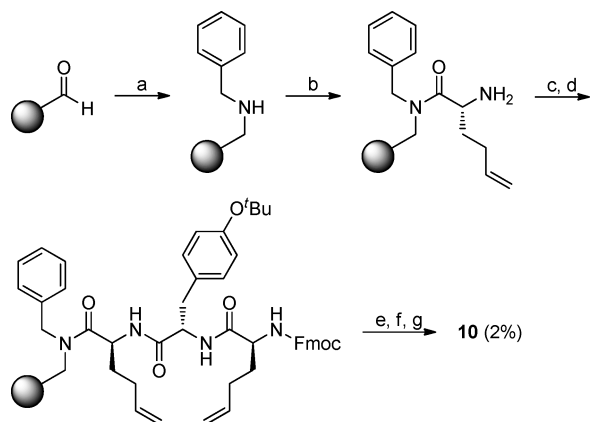
tetrachloro-1,4-benzoquinone was inefficient. Cyclization was effectively achieved under microwave heating at 120 or 140 °C for 5 min, using a lower amount of catalyst (0.07 equiv of HGII) in combination with BQ (0.15 equiv) and with DCE as solvent.

Both the *E* and *Z* isomers were obtained and isolated. The *E* olefin was consistently the predominant product (>60%).

Generally, the amino acids were single-coupled using 1-[bis(dimethylamino)methyliumyl]-1*H*-1,2,3-triazolo[4,5-*b*]pyridine-3-oxide

hexafluorophosphate (HATU) and *N,N*-diisopropylethylamine (DIEA) in DMF, with reaction times of 2 h for primary amines and overnight for secondary amines. Completeness of the coupling reactions was normally assessed by small scale cleavage and LCMS analysis. The existence of secondary amines was examined using

Scheme 2. Synthesis of 10 Using FMPB AM Resin^a



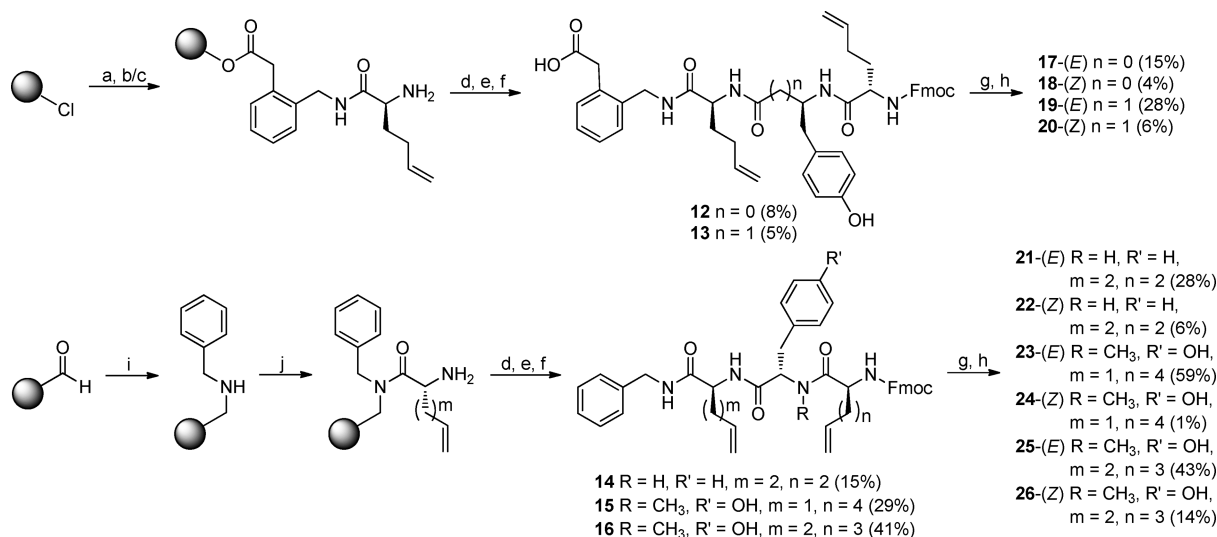
^a Reagents and conditions: (a) BA, NaBH(OAc)₃, AcOH/DMF (1:99), microwave, 60 °C, 20 min; (b) (i) Fmoc-Hag-OH, HATU, DIEA, DMF, room temp, on, (ii) 20% piperidine/DMF; (c) (i) Fmoc-Tyr(^tBu)-OH, 3-[bis(dimethylamino)methylumyl]-3*H*-benzotriazol-1-oxide hexafluorophosphate (HBTU), DIEA, DMF, room temp, 2 h; (d) (i) Fmoc-Hag-OH, HATU, DIEA, DMF, room temp, 2 h, (ii) 20% piperidine/DMF; (e) (i) HGII, DCE, microwave, 150 °C, 5 min, (ii) HGII, DCE, microwave, 150 °C, 5 min, (iii) DMSO, CH₂Cl₂, room temp, on, (iv) 20% piperidine/DMF; (f) TFA/TES/H₂O (90:5:5), room temp, 2 h; (g) H₂, Pd/C, EtOH, room temp, 1.5 h.

the chloranil test.^{63,64} Solid-phase Fmoc deprotection was accomplished with 20% piperidine in DMF. The coupling–deprotection cycle was repeated until the desired amino acid sequence had been synthesized.

As shown in Scheme 1, the synthesis of 7–9 started with *N,N'*-diisopropylcarbodiimide (DIC) mediated coupling of 2-(azidomethyl)phenylacetic acid to Wang resin. The subsequent coupling of homoallylglycine (Hag) was conducted by addition of tributylphosphine to a mixture of resin bound azide and activated amino acid in CH₂Cl₂.^{42,43,65} The remaining amino acids were coupled as described above. Purification and separation of the multiple products obtained upon cleavage from the resin after RCM and deprotection yielded 7. The remaining product mixtures were combined and subsequently reduced by catalytic hydrogenation to yield 8 and 9.

The synthesis of 10 started with the attachment of the C-terminal benzylamine (BA) moiety to FMPB AM resin through reductive amination utilizing NaBH(OAc)₃ in 1% AcOH/DMF (Scheme 2). The reaction was performed under microwave heating at 60 °C for 20 min.^{45,66} Standard couplings were used for the introduction of the three amino acid sequence. The attachment of BA and the initial coupling were monitored by colorimetric tests using the starting resins as references. The incidence of CHO groups was assessed using the *p*-anisaldehyde test,⁶⁷ and the existence of secondary amines was investigated using the chloranil test.^{63,64} The products obtained through on-resin RCM followed by deprotection and cleavage were purified and then converted to the corresponding saturated analogues by catalytic hydrogenation, giving two products separable by RP-HPLC. One product contained the desired 13-membered ring in the N-terminal part (10), and the other incorporated the corresponding ring-contracted 12-membered ring. The latter is

Scheme 3. Synthesis of 17–26 by RCM of the Corresponding Fmoc Protected Linear Intermediates 12–16, Which Were Synthesized Using 2-Chlorotrityl Chloride Resin or FMPB AM Resin^a



^a Reagents and conditions: (a) (i) 2-(azidomethyl)phenylacetic acid, DIEA, CH₂Cl₂, room temp, 4 h, (ii) MeOH, 15 min; (b) (i) PBu₃, DMF, (ii) Fmoc-Hag-OH, HATU, DIEA, DMF, room temp, on, (iii) 20% piperidine/DMF; (c) (i) Fmoc-Hag-OH, DIC, HOBT, CH₂Cl₂, (ii) PBu₃, room temp, on, (iii) 20% piperidine/DMF; (d) (i) Fmoc-Tyr(^tBu)-OH, Fmoc-β³hTyr(^tBu)-OH, Fmoc-Phe-OH or Fmoc-N-Me-Tyr(^tBu)-OH, HATU, DIEA, DMF, room temp, 2 h, (ii) 20% piperidine/DMF; (e) Fmoc-Hag-OH, (2*S*)-Fmoc-2-amino-6-heptenoic acid or (2*S*)-Fmoc-2-amino-7-octenoic acid (11), HATU, DIEA, DMF, room temp, 2 h for primary amines and overnight for secondary amines; (f) TFA/TES/H₂O (90:5:5), room temp, 2 h; (g) HGII, BQ, DCE, microwave, 120 or 140 °C, 5 min; (h) DBU, 3-mercaptopropyl functionalized silica gel, MeCN/DMF/DMSO, 30 min; (i) BA, NaBH(OAc)₃, AcOH/DMF (1:99), microwave, 60 °C, 20 min or 2 × 20 min; (j) (i) Fmoc-allylglycine (Fmoc-Alg-OH) or Fmoc-Hag-OH, HATU, DIEA, DMF, room temp, on, (ii) 20% piperidine/DMF.

not further discussed, as the structural assignment and evaluation were complicated by the low yield (<0.4 mg)

In the synthesis of **23** and **24**, (2*S*)-Fmoc-2-amino-7-octenoic acid (**11**) was required in the N-terminal position in the linear sequence (Scheme 3). It was obtained by transformation of the corresponding Boc-protected amino acid, which was commercially available. Removal of the *N*-Boc group with HCl in 1,4-dioxane gave the amine hydrochloride salt, which was neutralized and acylated by Fmoc-Cl under basic conditions (Supporting Information pp S6–S7).

The synthesis of analogues **17–20** (Scheme 3) was initiated by attachment of 2-(azidomethyl)phenylacetic acid⁴² to 2-chlorotriethyl chloride resin. The subsequent coupling of Fmoc-Hag-OH was conducted by addition of tributylphosphine to a mixture of resin bound azide and activated amino acid in CH₂Cl₂. The remaining amino acids were coupled as described above. The first two steps in the synthesis of analogues **21–26** (Scheme 3) were performed as described for analogue **10** (Scheme 2).

The Fmoc protected linear sequences were cleaved from the resin, purified by RP-HPLC, and subjected to RCM (**12–16**). The reaction was carried out in DCE under microwave heating at 120 or 140 °C for 5 min using HGII and BQ. Fmoc deprotection was performed using a few equivalents of 1,8-diazabicyclo-[5.4.0]undec-7-ene (DBU) in combination with 3-mercaptopropyl-functionalized silica gel as a dibenzofulvene scavenger.⁶⁸ To dissolve the lipophilic Fmoc protected compounds, DMF or DMSO (5–15%) was used in addition to CH₃CN. The reaction was completed in minutes, and after filtration and evaporation, the crude products were dissolved in appropriate mixtures of DMF/DMSO/CH₃CN/H₂O (0.1% TFA) and separated using RP-HPLC.

The double-bond configurations of the final compounds were established by primitive exclusive correlation spectroscopy (PE-COSY) and nuclear Overhauser effect spectroscopy (NOESY) experiments.^{69–71} The olefinic ³J_{HH} coupling constants were determined from the corresponding 2D PE-COSY spectra (³J_E = 15.2–18.0 Hz, ³J_Z = 8.5–14.2 Hz, Supporting Information Figure S1). Where extensive signal overlap of the *Z*-olefinic protons made the direct extraction of active couplings impossible, they were extracted as passive couplings from the cross-peaks to the neighboring methylene groups. The confirmation of the configurational assignment of the *E* isomers was provided by NOEs from the methylene protons on either side of the double bond to the olefinic protons (Supporting Information Figure S2).

Biochemical Evaluation. The ability of **7–10** and **17–26** to inhibit the catalytic activity of recombinant human IRAP and AP-N transiently transfected in HEK293 cells was examined and compared. Furthermore, the stability to degradation by metallo-peptidases in membrane homogenates was investigated for the majority of the analogues. To this end, membranes of endogenous IRAP-containing CHO-K1 cells were preincubated with different concentrations of compounds in the absence or presence of 5 mM 2-[2-[bis(carboxymethyl)amino]ethyl(carboxymethyl)amino]acetic acid (EDTA) and 100 μM 1,10-phenantroline (1,10-Phe), then further incubated with radioligand in the presence of both chelators. Because of the presence of the chelators during the binding step whether or not they were present during the preincubation, binding affinities solely refer to the IRAP apoenzyme.^{72–74} In this respect, similar removal of the catalytic zinc by the synergistic action of both chelators has also been observed to take place with AP-N, which like IRAP is also part of the M1 family of gluzincin aminopeptidases.⁷⁵ When the preincubation

proceeds in the absence of chelators, the competition curve will shift to the right (with respect to the situation in where the compound is exposed to the membranes in the continuous presence of the chelators), and the compound is quickly degraded by IRAP, AP-N, and/or other EDTA/1,10-Phe-sensitive metallo-peptidases. However, the absence of shift does not per se exclude potential degradation of the compound by alternative routes. The binding affinities and IRAP activity inhibition data of the compounds are presented in Table 1.

With a series of disulfide containing Ang IV analogues as starting points,⁴⁵ compounds with olefinic carbon bridges of *E* and *Z* configuration and more flexible saturated carbon bridges replacing the disulfide moiety were investigated. Compound **9** (Table 1), comprising a 13-membered macrocyclic system and a C-terminal AMPAA group, is only 3 times less efficient as an IRAP inhibitor ($K_i = 64.2$ nM) than the parent disulfide analogue **3** ($K_i = 22.5$ nM, Figure 1). The selectivity over AP-N is lower (i.e., $K_i(\text{AP-N})/K_i(\text{IRAP})$) and the stability somewhat higher as determined from binding affinity in the presence and absence of metal chelators. The less flexible *E* and *Z* olefin analogues **17** and **18** displayed similar results, i.e., a 2-fold lower IRAP activity than **3** ($K_i = 50.0$ and 41.1 nM, respectively), poorer selectivity, and slightly better stability. As with **9**, the C-terminally modified analogue **10** can be compared to the corresponding disulfide **4**. The 2-fold difference in IRAP activity between **10** ($K_i = 193$ nM) and **4** ($K_i = 95.7$ nM) is in accordance with the results obtained with **9** and **3**. The general trend is that the disulfide bridged analogues are more selective than the analogues comprising carbon–carbon bridges. To conclude, the replacement of a disulfide bridge by different carbon–carbon bridges is well tolerated in **3** and **4**, giving analogues **9**, **10**, **17**, and **18**, which suggests that there are similarities in the conformational properties between these 13-membered ring systems.

The importance of the C-terminal carboxyl group has been addressed previously (cf. **3** and **4**).⁴⁵ A 5-fold lower IRAP activity was observed for analogues where AMPAA was replaced by BA. Similar to the disulfides, a 3 times less potent IRAP inhibitor (**10**, $K_i = 193$ nM) was obtained by the same transformation of **9** ($K_i = 64.2$ nM). Generally, the γ -turn mimetic moiety AMPAA shows the best results, but it is evident that structural modifications are allowed in the C-terminal.

A one-carbon expansion of the 13-membered macrocycle of **9** resulted in a 2-fold potency increase (**8**, $K_i = 25.0$ nM). By introduction of a double bond in the resulting 14-membered ring system, a 6 times more potent inhibitor was obtained (**7**, $K_i = 4.1$ nM). Thus, a preference for 14-membered over 13-membered macrocycles was observed, indicating that the larger rings can adopt conformations different from those of the smaller rings upon interaction with IRAP.

Extension of the backbone by the insertion of β -amino acids influences the secondary structure by altering intramolecular interactions like hydrogen bonding, which sometimes leads to enhanced structural stability and β -amino acids acting as turn mimetics.^{77–79} Moreover, the proteolytic stability is frequently improved.^{39,80} The Tyr² residue was previously replaced by β ³H-Tyr, a modification that rendered potent ligands such as **5** and **6**.⁴⁵ By replacement of the Tyr residue in the 13-membered analogue **18** ($K_i = 41.1$ nM), a slightly more potent 14-membered analogue **20** ($K_i = 30.4$ nM) was obtained. When the same transformation was performed with the *E* isomer **17** ($K_i = 50.0$ nM), the most potent compound in this and previous series of Ang IV analogues was obtained, i.e., the 14-membered analogue

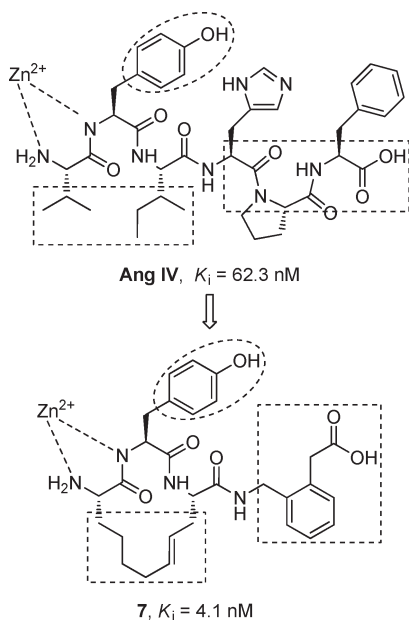


Figure 2. Proposed recognition elements of Ang IV and the Ang IV analogues (exemplified by **7**) important for IRAP interaction. Alternatively, the amide oxygen is coordinated to the catalytic zinc ion.

19 ($K_i = 1.8$ nM). Notably, while there was no difference in bioactivity with regard to the *E* and *Z* isomers **17** and **18**, a significant difference was seen in the case of the corresponding one-carbon enlarged *E* and *Z* isomers **19** and **20**, presumably due to more favorable conformational properties of **19**. Compared to analogue **7** ($K_i = 4.1$ nM), encompassing a 14-membered macrocycle with a differently located *E* olefin element and a Tyr instead of a β^3 hTyr residue, **19** is a 2-fold more potent IRAP inhibitor. Both analogues **19** and **7** were more stable than similar disulfides, but only **7** displayed similar selectivity for IRAP over AP-N (i.e., 1000-fold). The selectivity was 10 times lower for compound **19**.

The fact that the macrocyclic two-carbon analogues show improved stability compared to the substrate-like disulfides but not full stability in the CHO-K1 cells indicates that it is not only the disulfide bridge that makes the compounds susceptible to degradation.⁴⁵ Many reports on improved proteolytic stability, potency, selectivity, and membrane permeability of peptides and peptidomimetics have been attributed to mono- and multiple N-methylation of amino acid residues.^{77,81,82} It can also result in significant conformational changes due to altered configurational properties of the N-methylated peptide bonds bearing a sterically demanding methyl group, and a reduced number of hydrogen bond donors preventing intra- and intermolecular interactions. With the second best IRAP inhibitory effect and the best stability and selectivity over AP-N, **7** is one of the most promising compounds in the series. In order to investigate the importance of the NH group in the peptide bond between residues 1 and 2 and to potentially improve the stability, the Tyr² residue of the corresponding analogue incorporating BA in the C-terminus was subjected to N-methylation. This modification was found to have a significant impact on the activity (cf. **7** and **23**). However, part of the reduced activity is probably attributed to the lack of the C-terminal carboxyl group in **23** (cf. **9** and **10**). Since the analogue was devoid of all binding affinity, no conclusions could be drawn concerning its ability to resist degradation by metalloproteinases in CHO-K1 cells. A deleterious conformational impact

and a lack of proper coordination to the catalytic zinc ion by the amide nitrogen and possibly also by the oxygen are reasonable explanations of the outcome of the N-methylation of Tyr² in the cyclic Ang IV analogues (Figure 2).^{83–86} However, the amide oxygen has previously been shown not to be essential for high potency. Thus, Val-Ψ[CH₂NH]-Tyr-Val-Ψ[CH₂NH]-His-Pro-Phe (divalinal-Ang IV, $K_i = 194$ nM), incorporating a reduced peptide bond between residues 1 and 2 and between residues 3 and 4, is only 4 times less potent as an IRAP inhibitor compared to Ang IV.⁷³ The configuration of the double bond had a minor impact on the IRAP activity, while shifting of the double bond position one step away from the backbone resulted in a 2-fold decrease (c.f. **23–26**).

To assess the importance of the hydroxyl group, Tyr² was replaced by Phe. It is known that [Phe²]Ang IV (K_i of 1.00 nM) exhibits a slightly better binding affinity than Ang IV (K_i of 2.63 nM) to bovine adrenal membranes, as determined from the ability to compete with the binding of [¹²⁵I]Ang IV.³³ Its ability to inhibit IRAP has, to our knowledge, not been determined. In general, regarding the inhibitors encompassing 13-membered ring systems, no significant differences were observed when changing the type of two-carbon bridge. The outcome of **21** and **22** is in agreement with these observations. No more than a 2-fold difference was seen in activity between the *E* and *Z* isomers. On the basis of the above discussion, it is anticipated that **10** will be comparable to the corresponding unsaturated analogues. Consequently, since inhibitors **21** ($K_i = 697$ nM) and **22** ($K_i = 351$ nM) are respectively 2 and 4 times less active than **10** ($K_i = 193$ nM), the hydroxyl group seems to be beneficial but not a prerequisite for IRAP activity.

CONCLUSIONS

The design, synthesis, and biochemical evaluation of novel 13- and 14-membered macrocyclic tripeptide analogues of Ang IV are presented. It was demonstrated that the replacement of a disulfide bridge by a carbon–carbon bridge in the N-terminal macrocyclic part was well tolerated. The IRAP-inhibitory effects were in the same range as for the disulfides, and the stability to degradation by metalloproteinases was somewhat improved, while the selectivity over AP-N was reduced. A preference for 14-membered rings over 13-membered rings was observed. Generally, the type (saturated versus unsaturated), configuration, and position of the carbon–carbon bond did not have a considerable impact on the outcome. However, **7** (*E*) was superior to the saturated analogue **8**, and **19** (*E*) was found to be better than **20** (*Z*). Hence, the potency generally varied more with the type of macrocycle than with the specific characteristics of the carbon–carbon bond. Substitution of Tyr² by β^3 hTyr was well tolerated. Notably, N-methylation of Tyr² was deleterious to activity, conceivably because of the obstruction of coordination to the catalytic zinc ion or unfavorable conformational properties of these compounds. The most potent, selective, and stable analogues in the series, **7** ($K_i = 4.1$ nM) and **19** ($K_i = 1.8$ nM), serve as starting points for further optimization.

EXPERIMENTAL SECTION

General Information. Microwave heated reactions were performed in a Smith Synthesizer (Biotage AB, Uppsala, Sweden) producing controlled irradiation at 2450 MHz. Analytical RP-HPLC–MS was performed on a Gilson HPLC system with a Finnigan AQA quadrupole

mass spectrometer using an Onyx monolithic C18 column (4.6 mm × 50 mm) with gradients of CH₃CN/H₂O (0.05% HCOOH) or MeOH/H₂O (0.05% HCOOH) at a flow rate of 4 mL/min. Both UV (DAD, 214 and 254 nm) and MS (ESI) detection was utilized. Preparative RP-HPLC was performed using a Zorbax SB-C8 column (5 μm, 21.2 mm × 150 mm) with gradients of CH₃CN/H₂O (0.1% TFA) at a flow rate of 5 mL/min and UV detection at 230 nm. The purity of the compounds was determined on a Zorbax SB-C8 column (5 μm, 4.6 mm × 50 mm) and an Allure biphenyl column (5 μm, 4.6 mm × 50 mm) using the same buffer systems at a flow rate of 2 mL/min and with UV detection at 220 nm. A purity of more than 95% was established for all compounds with the exception of **18** (≥92.5%). NMR spectra were recorded on a Varian Mercury Plus spectrometer (¹H at 400 MHz and ¹³C at 101 MHz) and Varian INOVA spectrometers (¹H at 900, 800, or 600 MHz and ¹³C at 151 MHz) at ambient temperature. Chemical shifts (δ) are reported in ppm referenced indirectly to TMS via the ²H lock signal. Assignments were made using gCOSY, PE-COSY, TOCSY, NOESY, gHSQC, and gHMBC experiments. Mixing times between 0.4 and 0.6 s were used in NOESY experiments. PE-COSY spectra were acquired with 4096 × 2048 data points and zero-filled to 16384 × 8192 points for measurements of ³J_{HH}. The amino acid residues at positions 1 and 3 are denoted Xaa¹ and Xaa³, respectively. Exact molecular masses were determined on a Micromass Q-ToF2 mass spectrometer equipped with an electrospray ion source at the Department of Pharmaceutical Biosciences, Uppsala University, Sweden. The manual solid-phase synthesis was performed in disposable syringes fitted with porous polyethylene filters, and a Stuart SB2 tube rotator was used for agitation. The resins were purchased from Novabiochem and the unnatural amino acids from RSP Amino Acids or Sigma-Aldrich. The synthesis of 2-(azidomethyl)phenylacetic acid has been described earlier.⁴² Dichloromethane used in the reactions was distilled over calcium hydride. Other chemicals were purchased and used without further purification. Final product yields were determined based on the initial loading of the resin.

General Procedure A: Attachment of 2-(Azidomethyl)phenylacetic Acid to Wang Resin⁸⁷. Wang resin was added to a Biotage microwave vial and swollen in CH₂Cl₂/DMF (9:1) under gentle stirring for 30 min. A solution of 2-(azidomethyl)phenylacetic acid (2.0 equiv) and DIC (2.0 equiv) in CH₂Cl₂/DMF (9:1) was added, followed by DMAP (0.1 equiv) in CH₂Cl₂/DMF (9:1). After being sealed, the vial was flushed with nitrogen gas and the reaction mixture was heated to 44 °C in a heating block for 3 h, after which it was transferred to a 5 mL disposable syringe fitted with a porous polyethylene filter. The resin was washed with several portions of, in turn, CH₂Cl₂ and DMF. The remaining hydroxyl groups on the resin were capped using acetic anhydride (5.0 equiv) and pyridine (1.0 equiv) in DMF. After 30 min the resin was washed with several portions of, in turn, DMF, MeOH, and CH₂Cl₂ and then used directly in the subsequent step.

General Procedure B: Reductive Amination of FMPB AM Resin. FMPB AM resin, NaBH(OAc)₃ (5–10 equiv), and DMF were added to a 10–20 mL Biotage microwave vial. After being sealed, the vial was flushed with nitrogen gas, and BA (5–10 equiv), and AcOH (cat.) were added. The reaction mixture was heated to 60 °C by microwave irradiation for 20 min, cooled to room temperature, and then transferred to a 5 mL disposable syringe fitted with a porous polyethylene filter. The resin was washed with several portions of, in turn, DMF, MeOH, and CH₂Cl₂ and dried in vacuo. The reductive amination and washing were sometimes repeated once to ensure a sufficient yield. Two colorimetric tests were employed to examine the reaction, the *p*-anisaldehyde test for the presence of CHO groups⁶⁷ and the chloranil test^{63,64} for the presence of secondary amines. The FMPB AM resin was used as a reference.

General Procedure C: Attachment of 2-(Azidomethyl)phenylacetic Acid to 2-Chlorotrityl Chloride Resin. 2-(Azidomethyl)phenylacetic acid⁴² (1.0 equiv) was reacted with 2-chlorotrityl chloride resin (1.5 equiv) in CH₂Cl₂ in the presence of DIEA (4.0 equiv). After

5–7 h, MeOH was added, and the mixture was stirred for at least 15 min before the resin was transferred to a 5 mL disposable syringe fitted with a porous polyethylene filter. The resin was then washed with several portions of, in turn, CH₂Cl₂, DMF, MeOH, and CH₂Cl₂ and dried in vacuo.

General Procedure D: Coupling to 2-(Azidomethyl)phenylacetyl-2-chlorotrityl Resin Type 1. A round-bottomed flask was charged with the appropriate amino acid (1.1–1.5 equiv), HOBt (1.1–1.5 equiv), and DIC (1.1–1.5 equiv) in dry CH₂Cl₂. After preactivation under nitrogen for 10 min, the amino acid was treated with 2-(azidomethyl)phenylacetyl-2-chlorotrityl resin (1.0 equiv), followed 10 min later by PBu₃ (1.1–2.0 equiv). The reaction mixture was stirred under nitrogen for 6 h and then transferred to a 5 mL disposable syringe fitted with a porous polyethylene filter. The resin was washed with several portions of, in turn, CH₂Cl₂, DMF, MeOH, and CH₂Cl₂ and dried in vacuo.

General Procedure E: Coupling to 2-(Azidomethyl)phenylacetyl-2-chlorotrityl Resin Type 2. 2-(Azidomethyl)phenylacetyl-2-chlorotrityl resin was added to a round-bottomed flask, swollen in DMF under gentle stirring, treated with PBu₃ (1.2 equiv), followed 10 min later by a mixture of the appropriate amino acid (1.2 equiv), HATU (1.2 equiv), and DIEA (2.4 equiv) in DMF. The reaction mixture was stirred under nitrogen overnight and then transferred to a 5 mL disposable syringe fitted with a porous polyethylene filter. The resin was washed with several portions of, in turn, DMF, MeOH, and CH₂Cl₂ and dried in vacuo.

General Procedure F: Coupling and Deprotection of Amino Acids. Unless otherwise stated, a solution of the appropriate amino acid (1.1–3.0 equiv), HATU (1.1–3.0 equiv), and DIEA (2.2–6 equiv) in DMF was added to the resin and the reaction mixture was agitated by rotation for 2 h (primary amines) or overnight (secondary amines). After the resin was washed with several portions of DMF, the resin was treated with 20% piperidine in DMF (2 × 4 mL) to remove the Fmoc group and again rinsed thoroughly with DMF. Upon completion of the coupling cycle the resin was also washed with several portions of, in turn, CH₂Cl₂, MeOH, and CH₂Cl₂, and dried in vacuo.

General Procedure G: RCM on Resin and Fmoc Deprotection. The resin was transferred to a Biotage microwave vial (10–20 mL) and preswollen in DCE under nitrogen gas. A solution of HGII (0.15 equiv) in DCE was added, and the tube was sealed with a Teflon coated septa under air. The reaction mixture was heated to 140 or 150 °C by microwave irradiation for 5 min and then cooled to room temperature. A needle was used to relieve the pressure in the vial before the addition of a second portion of HGII (0.15 equiv) in DCE. The reaction mixture was heated to 140 or 150 °C for another 5 min, after which the resin was transferred to a 5 mL disposable syringe and washed with several portions of, in turn, CH₂Cl₂, DMF, and CH₂Cl₂. A mixture of DMSO (30 equiv) and CH₂Cl₂ was added to the resin. After rotation overnight the resin was washed with CH₂Cl₂ and DMF. Fmoc deprotection by treatment with 20% piperidine in DMF (2 × 4 mL) was followed by washing with several portions of, in turn, CH₂Cl₂, DMF, MeOH, and CH₂Cl₂ and drying in vacuo.

General Procedure H: Resin Cleavage, Side Chain Deprotection, and Purification. The resin was transferred to a 50 mL Falcon tube containing a stirring bar and treated with a mixture of 95% TFA (3.0 mL) and TES (0.2 mL) under gentle stirring for 2 h. The resin was filtered off and further washed with TFA, CH₃CN, CH₂Cl₂, and MeOH. The filtrate was evaporated, and the residue was dissolved in a mixture of DMSO/DMF/CH₃CN/H₂O (0.1% TFA) at appropriate ratios, filtered through a prerinsed cotton-plugged Pasteur pipet, and purified using RP-HPLC. Selected fractions were analyzed with HPLC–MS/UV, and those containing pure product were pooled and lyophilized.

General Procedure I: RCM in Solution, Fmoc Deprotection, and Purification. The starting material was weighed into a Biotage microwave vial (2–5 mL or 10–20 mL). A stirring bar was

added followed by DCE, and HGII (0.07 equiv) and the appropriate benzoquinone (0.15 equiv) dissolved in DCE (freshly prepared stock solutions). The tube was sealed with a Teflon coated septa under air. The reaction mixture was heated to 120 or 140 °C by microwave irradiation for 5 min and then cooled to room temperature. The reaction mixture was transferred to a round-bottomed flask, and the solvent was evaporated. If possible, the crude products were passed through a short RP column or precipitated in H₂O/CH₃CN/MeOH and separated by filtration. The residue was dissolved in DMSO/DMF/CH₃CN/H₂O (0.1% TFA), filtered through a prerinsed cotton-plugged Pasteur pipet, and purified using RP-HPLC. Selected fractions were analyzed using HPLC–MS/UV, and those containing pure product were pooled and lyophilized. 3-Mercaptopropyl functionalized silica gel (1.2 mmol/g, 5.0–10 equiv) was weighed into a disposable column, washed thoroughly with CH₃CN, and then transferred to a glass tube (25 mL). The purified Fmoc protected compound was dissolved in CH₃CN/DMF/DMSO (ratio adjusted to solubility) and added to the glass tube followed by DBU (2.5–5.0 equiv). The tube was sealed with a cap and rotated on a tube rotator. The reaction was monitored using analytical HPLC–MS/UV. After 30 min the reaction mixture was filtered through a prerinsed cotton-plugged Pasteur pipet into a round bottomed flask. The pH of the solution was adjusted to 4 using CH₃CN (0.1% TFA), and the residue remaining after evaporation was diluted with DMSO/DMF/CH₃CN/H₂O (0.1% TFA) with appropriate ratios, filtered through a prerinsed cotton-plugged Pasteur pipet, and purified using RP-HPLC. Selected fractions were analyzed using HPLC–MS/UV, and those containing pure product were pooled and lyophilized to give the pure product as the TFA salt.

General Procedure J: Catalytic Hydrogenation of Olefins.

A mixture of the macrocyclic olefins and 10% Pd/C in absolute ethanol was stirred under hydrogen gas at atmospheric pressure and room temperature for 1.5–4 h. After filtration through a disposable syringe filter and evaporation, the crude product(s) were purified using RP-HPLC.

Compounds 7, 8, and 9. Solid-phase attachment was performed according to general procedure A. Two batches were made using Wang resin (402 mg, 261 μmol), 2-(azidomethyl)phenylacetic acid (100 mg, 525 μmol), DIC (81 μL, 520 μmol), DMAP (3.8 mg, 31 μmol), CH₂Cl₂ (5.4 mL), and DMF (0.6 mL). Capping was achieved using acetic anhydride (123 μL, 1.31 mmol) and pyridine (21 μL, 261 μmol) in DMF (3.5 mL). The resin was then reacted with Fmoc-Hag-OH (273 mg, 776 μmol) as described in procedure D using HOBt (106 mg, 783 μmol), DIC (122 μL, 780 μmol), 85% PBU₃ (180 μL, 1.04 mmol), and CH₂Cl₂ (40 mL). Resin weight: 968 mg. Part of the resin (483 mg, 262 μmol) was then reacted with Fmoc-Tyr(^tBu)-OH (318 mg, 691 μmol) as described in procedure F using HATU (299 mg, 787 μmol) and DIEA (273 μL, 1.56 mmol) in DMF (3.0 mL). The same procedure was applied for the coupling of the N-terminal (2*S*)-Fmoc-2-amino-6-heptenoic acid (208 mg, 347 μmol) residue using HATU (110 mg, 302 μmol), DIEA (100 μL, 574 μmol), and DMF (3.0 mL). RCM was performed according to procedure G. The resin was preswollen in DCE (7.0 mL) for 1 h before the addition of 15 mol % HGII (23.7 mg, 37.8 μmol) in DCE (2.5 mL). An additional 15 mol % HGII (24.0 mg, 38.3 μmol) in DCE (2.5 mL) was added before the second round of heating. Workup using DMSO (543 μL, 7.61 mmol) and CH₂Cl₂ (3.5 mL) overnight was followed by Fmoc deprotection. Cleavage from the resin, following general procedure H, gave a mixture of products, i.e., ring-contracted and/or isomerized. The only compound separated in good yield by RP-HPLC was 7, with the double-bond shifted one step toward the backbone. The other compounds were pooled (4.8 mg, <7.5 μmol) and subjected to catalytic hydrogenation according to procedure J, using Pd/C (2.5 mg, 2.3 μmol) in absolute ethanol (2.0 mL).

2-(2-(((2*S*,5*S*,13*S*,*E*)-13-Amino-2-(4-hydroxybenzyl)-3,14-dioxo-1,4-diazacyclotetradec-7-ene-5-carboxamido)methyl)phenyl)acetic Acid (7). The product was isolated as the TFA salt

(2.79 mg, 2%). ¹H NMR (400 MHz, 0.1% TFA CD₃CN/D₂O 4:1) δ 7.27–7.18 (m, 3H, AMPAA-ArH), 7.14 (m, 1H, ArH), 7.04 (m, 2H, Tyr-H2, Tyr-H6), 6.67 (m, 2H, Tyr-H3, Tyr-H5), 5.25 (m, 1H, Xaa¹-H^ε), 5.16 (m, 1H, Xaa³-H^γ), 4.55 (dd, *J* = 8.3, 6.4 Hz, 1H, Tyr-H^α), 4.29 (dd, *J* = 10.1, 3.5 Hz, 1H, Xaa³-H^α), 4.25 (d, *J* = 15.4 Hz, 1H, AMPAA-NCH_{2a}), 4.19 (d, *J* = 15.4 Hz, 1H, AMPAA-NCH_{2b}), 3.81 (dd, *J* = 9.3, 4.3 Hz, 1H, Xaa¹-H^α), 3.67 (app s, 2H, AMPAA-CH₂CO), 2.92 (dd, *J* = 13.7, 8.3 Hz, 1H, Tyr-H^β), 2.79 (dd, *J* = 13.7, 6.4 Hz, 1H, Tyr-H^β), 2.40–2.33 (dm, 1H, Xaa³-H^β), 2.17 (ddd, *J* = 14.5, 10.1, 7.9 Hz, 1H, Xaa³-H^β), 1.94 (m, 2H, Xaa¹-H^ε, Xaa¹-H^{ε'}), 1.76 (m, 1H, Xaa¹-H^β), 1.58 (dddd, *J* = 13.5, 11.8, 9.3, 4.4 Hz, 1H, Xaa¹-H^β), 1.39–1.25 (m, 2H, Xaa¹-H^δ, Xaa¹-H^{δ'}), 1.17–0.98 (m, 2H, Xaa¹-H^γ, Xaa¹-H^{γ'}). ¹³C NMR (101 MHz, 0.1% TFA CD₃CN/D₂O 4:1) δ 175.3 (AMPAA-CO), 172.5 (Xaa³-CO), 171.8 (Tyr-CO), 170.0 (Xaa¹-CO), 156.4 (Tyr-C4), 137.6 (AMPAA-ArC), 134.8 (Xaa¹-C^ε), 133.6 (AMPAA-ArC), 131.8 (AMPAA-ArCH), 131.5 (Tyr-C2, Tyr-C6), 129.0 (AMPAA-ArCH), 128.58 (AMPAA-ArCH), 128.55 (AMPAA-ArCH), 128.47 (Tyr-C1), 127.4 (Xaa³-C^γ), 116.2 (Tyr-C3, Tyr-C5), 56.1 (Tyr-C^α), 53.9 (Xaa¹-C^α), 53.5 (Xaa³-C^α), 41.3 (AMPAA-NCH₂), 38.8 (AMPAA-CH₂CO), 37.2 (Tyr-C^β), 35.6 (Xaa³-C^β), 31.6 (Xaa¹-C^ε), 31.3 (Xaa¹-C^β), 27.5 (Xaa¹-C^δ), 23.0 (Xaa¹-C^γ). HPLC purity: C8 column 99.2%, biphenyl column 99.4%. HRMS (M + H⁺): 537.2718, C₂₉H₃₇N₄O₆ requires 537.2713. ³*J*_E = 15.6 Hz, measured from PE-COSY spectrum (DMSO-*d*₆).

2-(2-(((5*S*,8*S*,12*S*)-5,12-Di(but-3-en-1-yl)-1-(9*H*-fluoren-9-yl)-8-(4-hydroxybenzyl)-3,6,10,13-tetraoxo-2-oxa-4,7,11,14-tetraazapentadecan-15-yl)phenyl)acetic Acid (13). Solid-phase attachment was done according to general procedure C using 2-(azidomethyl)phenylacetic acid (101 mg, 528 μmol), 2-chlorotriethyl chloride resin (544 mg, 767 μmol), DIEA (350 μL, 2.02 mmol), and CH₂Cl₂ (6.0 mL). MeOH (0.6 mL) was added after 5 h, and the stirring was continued for 15 min. Resin weight: 612 mg. Part of the resin (604 mg, 520 μmol) was then reacted with Fmoc-Hag-OH (201 mg, 573 μmol) as described in procedure E using HOBt (77.3 mg, 572 μmol), DIC (81 μL, 517 μmol), 85% PBU₃ (99 μL, 571 μmol), and DMF (11 mL). The subsequent coupling of Fmoc-β³hTyr(^tBu)-OH (578 mg, 587 μmol) was performed with HATU (218 mg, 572 μmol) and DIEA (199 μL, 1.14 mmol) in DMF (3 mL) following general method F. This method was also applied for the coupling of the N-terminal amino acid Fmoc-Hag-OH (101 mg, 287 μmol) using HATU (110 mg, 290 μmol) and DIEA (99.7 μL, 572 μmol) in DMF (3 mL). Cleavage from the resin and purification, as described in procedure H, gave 13 as a white solid (18.6 mg, 5%). ¹H NMR (400 MHz, DMSO-*d*₆) δ 12.34 (br s, 1H, AMPAA-COOH), 9.12 (s, 1H, β³hTyr-OH), 8.28 (m, 1H, AMPAA-NH), 8.04 (d, *J* = 7.9 Hz, 1H, Hag³-NH), 7.89 (m, 2H, Fmoc-H4, Fmoc-H5), 7.77 (d, *J* = 7.8 Hz, 1H, β³hTyr-NH), 7.73 (m, 2H, Fmoc-H1, Fmoc-H8), 7.44 (d, *J* = 8.4 Hz, Hag¹-NH), 7.41 (m, 2H, Fmoc-H3, Fmoc-H6), 7.32 (m, 2H, Fmoc-H2, Fmoc-H7), 7.20–7.18 (m, 4H, AMPAA-ArH), 6.95 (m, 2H, β³hTyr-H2, β³hTyr-H6), 6.62 (m, 2H, β³hTyr-H3, β³hTyr-H5), 5.77 (dddd, *J* = 17.2, 10.0, 6.4, 6.4 Hz, 1H, Hag¹-H^δ/Hag³-H^δ), 5.74 (dddd, *J* = 17.2, 10.0, 6.4, 6.4 Hz, 1H, Hag¹-H^δ/Hag³-H^δ), 4.97 (dd, *J* = 17.2, 2.0 Hz, 1H, Hag¹-H^ε/Hag³-H^ε), 4.96 (dd, *J* = 17.2, 1.8 Hz, 1H, Hag¹-H^ε/Hag³-H^ε), 4.93 (m, 2H, Hag¹-H^{ε'}, Hag³-H^{ε'}), 4.34–4.19 (m, 6H, AMPAA-NCH₂, Hag³-H^α, Fmoc-CH₂, Fmoc-H9), 4.17 (m, 1H, β³hTyr-H^β), 3.89 (ddd, *J* = 8.9, 8.4, 5.3 Hz, 1H, Hag¹-H^α), 3.64 (app s, 2H, AMPAA-CH₂CO), 2.63 (dd, *J* = 13.7, 5.8 Hz, 1H, β³hTyr-H^γ), 2.58 (dd, *J* = 13.7, 6.8 Hz, 1H, β³hTyr-H^{γ'}), 2.31 (dd, *J* = 14.7, 6.6 Hz, 1H, β³hTyr-H^α), 2.25 (dd, *J* = 14.7, 6.8 Hz, 1H, β³hTyr-H^{α'}), 2.06–1.88 (m, 4H, Hag¹-H^γ, Hag¹-H^{γ'}, Hag³-H^γ, Hag³-H^{γ'}), 1.74 (m, 1H, Hag³-H^β), 1.66–1.49 (m, 3H, Hag³-H^{β'}, Hag¹-H^β, Hag¹-H^{β'}). ¹³C NMR (101 MHz, DMSO-*d*₆) δ 172.5 (AMPAA-CO), 171.6 (Hag³-CO), 171.0 (Hag¹-CO), 170.1 (β³hTyr-CO), 155.8 (Fmoc-CO), 155.6 (β³hTyr-C4), 144.0 (Fmoc-C8a/Fmoc-C9a), 143.8 (Fmoc-C8a/Fmoc-C9a), 140.7 (Fmoc-C4a, Fmoc-C4b), 137.9 (Hag¹-C^δ/Hag³-C^δ), 137.8 (Hag¹-C^δ/Hag³-C^δ), 137.7 (AMPAA-ArC), 132.9 (AMPAA-ArC),

130.5 (AMPAA-ArCH), 130.3 ($\beta^3\text{hTyr-C2}$, $\beta^3\text{hTyr-C6}$), 128.4 ($\beta^3\text{hTyr-C1}$), 127.6 (Fmoc-C3, Fmoc-C6), 127.4 (AMPAA-ArCH), 127.1 (Fmoc-C2, Fmoc-C7), 126.8 (AMPAA-ArCH), 126.7 (AMPAA-ArCH), 125.3 (Fmoc-C1, Fmoc-C8), 120.1 (Fmoc-C4, Fmoc-C5), 115.1 ($\text{Hag}^1\text{-C}^\epsilon/\text{Hag}^3\text{-C}^\epsilon$), 115.0 ($\text{Hag}^1\text{-C}^\epsilon/\text{Hag}^3\text{-C}^\epsilon$), 114.8 ($\beta^3\text{hTyr-C3}$, $\beta^3\text{hTyr-C5}$), 65.6 (Fmoc-CH₂), 54.3 ($\text{Hag}^1\text{-C}^\alpha$), 52.2 ($\text{Hag}^3\text{-C}^\alpha$), 47.9 ($\beta^3\text{hTyr-C}^\beta$), 46.7 (Fmoc-C9), 39.6 (AMPAA-NCH₂), 39.3 ($\beta^3\text{hTyr-C}^\alpha$), 38.4 ($\beta^3\text{hTyr-C}^\gamma$), 38.0 (AMPAA-CH₂CO), 31.2 ($\text{Hag}^1\text{-C}^\beta/\text{Hag}^3\text{-C}^\beta$), 31.1 ($\text{Hag}^1\text{-C}^\beta/\text{Hag}^3\text{-C}^\beta$), 29.26 ($\text{Hag}^1\text{-C}^\gamma/\text{Hag}^3\text{-C}^\gamma$), 29.56 ($\text{Hag}^1\text{-C}^\gamma/\text{Hag}^3\text{-C}^\gamma$), 29.56 ($\text{Hag}^1/\text{Hag}^3\text{-C}^\gamma$). HPLC purity: C8 column 99.6%, biphenyl column 99.2%. HRMS ($M + H^+$): 787.3702, C₄₆H₅₁N₄O₈ requires 787.3707.

(9H-Fluoren-9-yl)methyl ((S)-1-(((S)-1-(((S)-1-(Benzylamino)-1-oxopent-4-en-2-yl)amino)-3-(4-hydroxyphenyl)-1-oxopropan-2-yl)(methyl)amino)-1-oxooct-7-en-2-yl)carbamate (15). Solid-phase attachment was done according to general procedure B using FMPB AM resin (332 mg, 332 μmol), BA (328 μL , 3.00 mmol), NaBH(OAc)₃ (632 mg, 2.98 mmol), AcOH (0.04 mL), and DMF (4.50 mL). The reductive amination was repeated once using BA (164 μL , 1.50 mmol), NaBH(OAc)₃ (315 mg, 1.49 mmol), AcOH (0.05 mL), and DMF (8.00 mL). The subsequent couplings were accomplished following general method F. The resin was reacted with Fmoc-Alg-OH (125 mg, 370 μmol) using HATU (143 mg, 377 μmol), DIEA (127 μL , 729 μmol), and DMF (3 mL). The coupling of Fmoc-N-Me-Tyr(^tBu)-OH (173 mg, 366 μmol) was performed with HATU (139 mg, 366 μmol) and DIEA (127 μL , 729 μmol) in DMF (3.0 mL), and the N-terminal amino acid (2S)-Fmoc-2-amino-7-octenoic acid (92.7 mg, 244 μmol) was also introduced by coupling with HATU (109 mg, 287 μmol) and DIEA (127 μL , 729 μmol) in DMF (3 mL). Cleavage from the resin and purification, as described in procedure H, gave **15** as a white solid (72.0 mg, 29%). HPLC purity: C8 column 99.0%, biphenyl column 99.0%. HRMS ($M + H^+$): 743.3807, C₄₅H₅₁N₄O₆ requires 743.3809.

Compounds 19 and 20. Procedure I was applied for the synthesis of **19** and **20** starting from **13**. RCM was performed using **13** (14.6 mg, 18.6 μmol), HGII (0.73 mg, 1.16 μmol), and BQ (0.27 mg, 2.50 μmol) in DCE (5.5 mL). The ratios of ring-contracted product/*E* isomer/*Z* isomer were 1:6:2 as determined from HPLC–UV. The compounds were separated by RP-HPLC and subjected to Fmoc deprotection in approximately 15% DMSO/MeCN using DBU (5 equiv) and 3-mercaptopropyl functionalized silica gel (10 equiv). Purification by RP-HPLC gave **19** and **20** as white solids.

2-(2-(((2S,6S,13S,E)-13-Amino-2-(4-hydroxybenzyl)-4,14-dioxo-1,5-diazacyclotetradec-9-ene-6-carboxamido)methyl)phenyl)acetic Acid (19). The product was isolated as the TFA salt (3.4 mg, 28%, 1% overall). ¹H NMR (600 MHz, DMSO-*d*₆) δ 12.34 (br s, 1H, AMPAA-COOH), 9.23 (s, 1H, $\beta^3\text{hTyr-OH}$), 8.36 (d, *J* = 7.7 Hz, 1H, $\beta^3\text{hTyr-NH}$), 8.21 (m, 1H, AMPAA-NH), 8.13 (d, *J* = 7.6 Hz, 1H, Xaa³-NH), 8.05 (d, *J* = 5.6 Hz, 3H, Xaa¹-NH₃⁺), 7.20–7.17 (m, 4H, AMPAA-ArH), 7.04 (m, 2H, $\beta^3\text{hTyr-H2}$, $\beta^3\text{hTyr-H6}$), 6.69 (m, 2H, $\beta^3\text{hTyr-H3}$, $\beta^3\text{hTyr-H5}$), 5.42 (m, 1H, Xaa¹-H ^{δ}), 5.33 (m, 1H, Xaa³-H ^{δ}), 4.22 (m, 2H, AMPAA-NCH₂), 4.19 (m, 1H, $\beta^3\text{hTyr-H}^\beta$), 3.98 (dd, *J* = 14.7, 7.4 Hz, 1H, Xaa³-H ^{α}), 3.83 (m, 1H, Xaa¹-H ^{α}), 3.63 (app s, 2H, AMPAA-CH₂CO), 2.90 (dd, *J* = 13.5, 5.7 Hz, 1H, $\beta^3\text{hTyr-H}^\gamma$), 2.73 (dd, *J* = 13.8, 7.7 Hz, 1H, $\beta^3\text{hTyr-H}^\gamma$), 2.70 (dd, *J* = 14.8, 5.0 Hz, 1H, $\beta^3\text{hTyr-H}^\alpha$), 2.15 (m, 1H, Xaa³-H ^{γ}), 2.10 (dd, *J* = 14.8, 8.1 Hz, 1H, $\beta^3\text{hTyr-H}^\alpha$), 1.91–1.79 (m, 3H, Xaa¹-H ^{γ} , Xaa¹-H ^{γ'} , Xaa³-H ^{γ'}), 1.72–1.61 (m, 4H, Xaa¹-H ^{β} , Xaa¹-H ^{β'} , Xaa³-H ^{β} , Xaa³-H ^{β'}). ³J_E = 17.1 Hz, measured from PE-COSY spectrum. ¹³C NMR (151 MHz, DMSO-*d*₆) δ 172.5 (CO), 172.2 (CO), 170.7 (CO), 167.6 (CO), 155.9 ($\beta^3\text{hTyr-C4}$), 137.8 (AMPAA-ArC), 132.9 (AMPAA-ArC), 130.4 ($\beta^3\text{hTyr-C2}$, $\beta^3\text{hTyr-C6}$, AMPAA-ArCH), 129.5 (Xaa¹-C ^{δ}), 129.4 (Xaa³-C ^{δ}), 128.2 ($\beta^3\text{hTyr-C1}$), 127.2 (AMPAA-ArCH), 126.7 (AMPAA-ArCH), 126.6 (AMPAA-ArCH), 115.0 ($\beta^3\text{hTyr-C3}$, $\beta^3\text{hTyr-C5}$), 51.6 (Xaa¹-C ^{α}), 51.4 (Xaa³-C ^{α}), 49.2 ($\beta^3\text{hTyr-C}^\beta$), 39.7 ($\beta^3\text{hTyr-C}^\gamma$), 39.6 (AMPAA-NCH₂), 38.2

($\beta^3\text{hTyr-C}^\alpha$), 38.0 (AMPAA-CH₂CO), 31.1 (Xaa¹-C ^{β} /Xaa³-C ^{β}), 30.4 (Xaa³-C ^{β} /Xaa¹-C ^{β}), 22.6 (Xaa³-C ^{γ}), 21.1 (Xaa¹-C ^{γ}). HPLC purity: C8 column 99.0%, biphenyl column 99.4%. HRMS ($M + H^+$): 537.2711, C₂₉H₃₇N₄O₆ requires 537.2713.

Compounds 23 and 24. Procedure I was applied for the synthesis of **23** and **24** starting from **15**. RCM was performed using **15** (65.2 mg, 87.8 μmol), HGII (3.51 mg, 5.60 μmol), and BQ (1.42 mg, 13.2 μmol) in DCE (15 mL). Purification by RP-HPLC (53.9 mg, 75.4 μmol) was followed by Fmoc deprotection in 10% DMF/MeCN using DBU (2.5 equiv) and 3-mercaptopropyl functionalized silica gel (5.0 equiv). Separation by RP-HPLC gave the *E* and *Z* isomers, **23** and **24**, as white solids.

(2S,5S,13S,E)-13-Amino-N-benzyl-2-(4-hydroxybenzyl)-1-methyl-3,14-dioxo-1,4-diazacyclotetradec-7-ene-5-carboxamide (23). The product was isolated as the TFA salt (31.4 mg, 59%, 16% overall). ¹H NMR (600 MHz, DMSO-*d*₆) δ 9.25 (br s, 1H, Tyr-OH), 8.14 (d, *J* = 7.9 Hz, 1H, Xaa³-NH), 8.10 (m, 3H, Xaa¹-NH₃⁺), 7.73 (dd, *J* = 6.5, 5.6 Hz, 1H, BA-NH), 7.31 (m, 2H, BA-H3, BA-H5), 7.24 (m, 1H, BA-H4), 7.19 (m, 2H, BA-H2, BA-H6), 6.99 (m, 2H, Tyr-H2, Tyr-H6), 6.62 (m, 2H, Tyr-H3, Tyr-H5), 5.28 (m, 1H, Xaa¹-H ^{ϵ}), 5.20 (dd, *J* = 9.6, 5.1 Hz, 1H, Tyr-H ^{α}), 5.15 (m, 1H, Xaa³-H ^{γ}), 4.41 (m, 1H, Xaa¹-H ^{α}), 4.28 (dd, *J* = 15.3, 6.5 Hz, 1H, BA-NCH_{2a}), 4.22 (ddd, *J* = 11.8, 7.9, 3.5 Hz, 1H, Xaa³-H ^{α}), 4.09 (dd, *J* = 15.3, 5.6 Hz, 1H, BA-NCH_{2b}), 3.15 (dd, *J* = 13.6, 9.6 Hz, 1H, Tyr-H ^{β}), 2.95 (s, 3H, Tyr-NCH₃), 2.50 (m, 1H, Tyr-H ^{β'}), 2.45 (m, 1H, Xaa³-H ^{β}), 2.17 (ddd, *J* = 14.4, 11.8, 9.4 Hz, 1H, Xaa³-H ^{β'}), 2.06 (m, 1H, Xaa¹-H ^{ϵ}), 1.88 (m, 1H, Xaa¹-H ^{ϵ'}), 1.80 (m, 1H, Xaa¹-H ^{β}), 1.52 (m, 1H, Xaa¹-H ^{β'}), 1.34 (m, 1H, Xaa¹-H ^{δ}), 1.27 (m, 2H, Xaa¹-H ^{δ'} , Xaa¹-H ^{γ'}), 1.08 (m, 1H, Xaa¹-H ^{γ'}). ³J_E = 15.4 Hz, measured from PE-COSY spectrum. ¹³C NMR (151 MHz, DMSO-*d*₆) δ 171.0 (CO), 168.7 (CO), 168.4 (CO), 155.8 (Tyr-C4), 139.0 (BA-C1), 133.0 (Xaa¹-C ^{ϵ}), 129.9 (Tyr-C2, Tyr-C6), 128.2 (BA-C3, BA-C5), 127.3 (Tyr-C1), 127.0 (Xaa³-C ^{γ}), 126.9 (BA-C2, BA-C6), 126.7 (BA-C4), 115.0 (Tyr-C3, Tyr-C5), 57.1 (Tyr-C ^{α}), 53.0 (Xaa¹-C ^{α}), 49.2 (Xaa³-C ^{α}), 42.0 (BA-NCH₂), 34.4 (Xaa³-C ^{β}), 33.0 (Tyr-C ^{β}), 30.6 (Tyr-NCH₃), 30.4 (Xaa¹-C ^{ϵ} , Xaa¹-C ^{β}), 27.0 (Xaa¹-C ^{δ}), 20.8 (Xaa¹-C ^{γ}). HPLC purity: C8 column >99.9%, biphenyl column 99.8%. HRMS ($M + H^+$): 493.2804, C₂₈H₃₇N₄O₄ requires 493.2815.

Biochemical Evaluation. L-Leucine-*p*-nitroanilide (L-Leu-pNA) was obtained from Sigma-Aldrich. [³H]AL-11 was obtained from G. Tóth, Biological Research Center (Szeged, Hungary).⁷⁶ All other reagents were of the highest grade commercially available. CHO-K1 cells were kindly donated by the Pasteur Institute (Brussels, Belgium).

Cell Culture, Transient Transfection, and Membrane Preparation. CHO-K1 and HEK293 cell lines were cultured in 75 and 500 cm² culture flasks in Dulbecco's modified essential medium (DMEM) supplemented with L-glutamine (2 mM), 2% (v/v) of a stock solution containing 5000 IU/mL penicillin and 5000 $\mu\text{g}/\text{mL}$ streptomycin (Invitrogen, Merelbeke, Belgium), 1% (v/v) of a stock solution containing nonessential amino acids, 1 mM sodium pyruvate, and 10% (v/v) fetal bovine serum (Invitrogen, Merelbeke, Belgium). The cells were grown in 5% CO₂ at 37 °C until confluent.

HEK293 cells were transiently transfected with plasmid DNA, with pCIneo containing the gene of human IRAP (kindly provided by Prof. M. Tsujimoto, Laboratory of Cellular Biochemistry, Saitama, Japan) or pTEJ4⁸⁸ carrying the complete human AP-N cDNA.²⁵ The transient transfection was performed as described previously with 8 $\mu\text{L}/\text{mL}$ Lipofectamine (Invitrogen, Merelbeke, Belgium) and 1 $\mu\text{g}/\text{mL}$ plasmid DNA.⁸⁹ After transfection, the cells were cultured for 2 more days. IRAP and AP-N transfected HEK293 cells displayed a 10 and 8 times higher enzyme activity, respectively, than nontransfected cells.

CHO-K1 cell and transfected HEK293 cell membranes were prepared as described previously.⁹⁰ Briefly, the cells were harvested with 0.2% EDTA (w/v) (in phosphate buffered saline (PBS), pH 7.4) and centrifuged for 5 min at 500g at room temperature. After resuspension in

PBS, the cells were counted and washed. The cells were then homogenized in 50 mM Tris-HCl (at pH 7.4) using a Polytron homogenizer (10 s at maximum speed) and a Potter homogenizer (30 strokes at 1000 rpm) and then centrifuged for 30 min (30000g at 4 °C). The pellet was resuspended in 50 mM Tris-HCl and centrifuged (30 min 30000g at 4 °C), and the supernatant was removed. The resulting pellets were stored at -20 °C until use.

Enzyme Assay. Determination of the aminopeptidase catalytic activity was based on the cleavage of the substrate L-leucine-*p*-nitroanilide (L-Leu-pNA)⁹⁰ to give L-leucine and *p*-nitroaniline. This latter compound displays a characteristic light absorption maximum at 405 nm. Pellets, prepared as described above, were thawed and resuspended using a Polytron homogenizer in enzyme assay buffer containing 50 mM Tris-HCl (pH 7.4), 140 mM NaCl, 0.1% (w/v) bovine serum albumin (BSA), and 100 μM phenylmethylsulfonyl fluoride (PMSF). The incubation mixture comprised 50 μL of membrane homogenate, 200 μL of L-Leu-pNA (1.5 mM), and 50 μL of enzyme assay buffer alone or with the test compound. The amount of membrane homogenate corresponded to 1.5×10^5 transfected HEK293 cells in each well. Assays were carried out at 37 °C in 96-well plates (Medisch Labo Service, Menen, Belgium), and the formation of *p*-nitroaniline was monitored by measuring the absorption at 405 nm every 5 min between 10 and 50 min in a Tecan M200 96-well reader. The enzymatic activities were calculated by linear regression analysis of the timewise increase in absorption.

Stability Experiments. The stability of the compounds was studied in the presence of CHO-K1 cell membranes. Membrane pellets were thawed and resuspended using a Polytron homogenizer in 50 mM Tris-HCl (pH 7.4) enzyme assay buffer. Preincubations were carried out for 40 min at 37 °C in a final volume of 250 μL containing 150 μL of membrane homogenate (corresponding to 4×10^5 CHO-K1 cells, 50 μL of enzyme assay buffer without or with 30 mM EDTA/600 μM, 1,10-Phe, and 50 μL of enzyme assay buffer without or with the different compounds or unlabeled Ang IV (60 μM for nonspecific binding). Then the binding assay was initiated by adding 50 μL of enzyme assay buffer containing [³H]AL-11 (18 nM, without (if chelators were already present in the preincubation medium) or with 30 mM EDTA/600 μM 1,10-Phe), and the mixture was further incubated for 30 min at 37 °C. The final chelator concentrations were 5 mM EDTA and 100 μM 1,10-Phe. The [³H]AL-11 concentration was 3 nM, and the final unlabeled ligand concentrations ranged from 10^{-5} to 10^{-9} M. After incubation, the mixture was vacuum-filtered using an Inotech 24-well cell harvester through GF/B glass fiber filters (Whatman) presoaked in 1% (w/v) BSA. After the filters were dried, the radioactivity retained by the filters was measured (after adding 3 mL of scintillation liquid (Optiphase Hisafe)) using a β-counter (Perkin-Elmer). [³H]AL-11 was characterized as described by Demaegdts et al.⁷⁶

Data Analysis. All experiments were performed at least twice with duplicate determinations in each experiment. The calculation of IC₅₀ from competition binding (or enzyme inhibition) experiments was performed by nonlinear regression analysis using GraphPad Prism, version 5.0. The equilibrium dissociation constants (*K*_i) of the tested compounds in the binding and enzyme assays were calculated using the equation $K_i = [IC_{50}/(1 + [L]/K)]$ in which [L] is the concentration of the free radioligand (binding) or free substrate concentration (enzyme assay) and *K* the equilibrium dissociation constant (KD) of [³H]AL-11 (from saturation binding experiments) or the Michaelis–Menten constant (*K*_m) for substrate cleavage.⁹¹

■ ASSOCIATED CONTENT

Supporting Information. Additional synthetic and analytical data. This material is available free of charge via the Internet at <http://pubs.acs.org>.

■ AUTHOR INFORMATION

Corresponding Author

*Phone: +46 18 4714284. Fax: +46 18 4714474. E-mail: Anders.Hallberg@orgfarm.uu.se.

■ ACKNOWLEDGMENT

We gratefully acknowledge The Swedish Research Council for economic support. H.D. was a postdoctoral researcher of the “Fund for Scientific Research—Flanders” (FWO, Belgium). We are grateful to Prof. D. Tourwé and A. Lukaszuk (Department of Organic Chemistry, Vrije Universiteit Brussel, Belgium) for the preparation of the AL-11 precursor and to G. Tóth and E. Szemenyei (Biological Research Center, Szeged, Hungary) for the tritiation of this precursor to [³H]AL-11.⁶ We also thank Aleh Yahorau for conducting the HRMS experiments.

■ ABBREVIATIONS USED

Alg, allylglycine, (2*S*)-2-amino-4-pentenoic acid; AMPAA, 2-(amino-methyl)phenylacetic acid; Ang IV, angiotensin IV; AP-N, aminopeptidase N; BA, benzylamine; BQ, 1,4-benzoquinone; DBU, 1,8-diazabicyclo[5.4.0]undec-7-ene; DCE, 1,2-dichloroethane; DIC, *N,N'*-diisopropylcarbodiimide; DIEA, *N,N*-diisopropylethylamine; EDTA, 2-[2-[bis(carboxymethyl)amino]ethyl(carboxymethyl)amino]acetic acid; Fmoc, 9-fluorenylmethoxycarbonyl; FMPB AM, 4-(4-formyl-3-methoxyphenoxy)butyrylaminoethyl; GII, Grubbs catalyst second generation, benzylidene[1,3-bis-(2,4,6-trimethylphenyl)-2-imidazolidinylidene]dichloro(tricyclohexylphosphine)ruthenium; Hag, homoallylglycine, (2*S*)-2-amino-5-hexenoic acid; HATU, 1-[bis(dimethylamino)methyliumyl]-1*H*-1,2,3-triazolo[4,5-*b*]pyridine-3-oxide hexafluorophosphate; HBTU, 3-[bis(dimethylamino)methyliumyl]-3*H*-benzotriazol-1-oxide hexafluorophosphate; HGII, Hoveyda–Grubbs catalyst second generation, (1,3-bis-(2,4,6-trimethylphenyl)-2-imidazolidinylidene)dichloro(*o*-isopropoxyphenylmethylene)ruthenium; HOBt, 1-hydroxybenzotriazole; IRAP, insulin-regulated aminopeptidase; NOESY, nuclear Overhauser effect spectroscopy; PE-COSY, primitive exclusive correlation spectroscopy; RCM, ring-closing metathesis; RAS, renin–angiotensin system; TES, triethylsilane; TFA, trifluoroacetic acid; Xaa¹, amino acid residue at position 1; Xaa³, amino acid residue at position 3

■ REFERENCES

- (1) Albiston, A. L.; Pederson, E. S.; Burns, P.; Purcell, B.; Wright, J. W.; Harding, J. W.; Mendelsohn, F. A.; Weisinger, R. S.; Chai, S. Y. Attenuation of scopolamine-induced learning deficits by LVV-hemorphin-7 in rats in the passive avoidance and water maze paradigms. *Behav. Brain Res.* **2004**, *154*, 239–243.
- (2) Braszko, J. J. Dopamine D4 receptor antagonist L745,870 abolishes cognitive effects of intracerebroventricular angiotensin IV and des-Phe⁶-Ang IV in rats. *Eur. Neuropsychopharmacol.* **2009**, *19*, 85–91.
- (3) Braszko, J. J.; Wlasienko, J.; Koziolkiewicz, W.; Janecka, A.; Wisniewski, K. The 3-7 fragment of angiotensin II is probably responsible for its psychoactive properties. *Brain Res.* **1991**, *542*, 49–54.
- (4) Braszko, J. J.; Kupryszewski, G.; Witczuk, B.; Wisniewski, K. Angiotensin II-(3-8)-hexapeptide affects motor activity, performance of passive avoidance and a conditioned avoidance response in rats. *Neuroscience* **1988**, *27*, 777–783.
- (5) Golding, B. J.; Overall, A. D.; Brown, G.; Gard, P. R. Strain differences in the effects of angiotensin IV on mouse cognition. *Eur. J. Pharmacol.* **2010**, *641*, 154–159.

- (6) Kramar, E. A.; Armstrong, D. L.; Ikeda, S.; Wayner, M. J.; Harding, J. W.; Wright, J. W. The effects of angiotensin IV analogs on long-term potentiation within the CA1 region of the hippocampus in vitro. *Brain Res.* **2001**, *897*, 114–121.
- (7) Lee, J.; Albiston, A. L.; Allen, A. M.; Mendelsohn, F. A.; Ping, S. E.; Barrett, G. L.; Murphy, M.; Morris, M. J.; McDowall, S. G.; Chai, S. Y. Effect of I.C.V. injection of AT₄ receptor ligands, Nle¹-angiotensin IV and LVV-hemorphin 7, on spatial learning in rats. *Neuroscience* **2004**, *124*, 341–349.
- (8) Lee, J.; Chai, S. Y.; Mendelsohn, F. A.; Morris, M. J.; Allen, A. M. Potentiation of cholinergic transmission in the rat hippocampus by angiotensin IV and LVV-hemorphin-7. *Neuropharmacology* **2001**, *40*, 618–623.
- (9) Olson, M. L.; Cero, I. J. Intrahippocampal norleucine¹-angiotensin IV mitigates scopolamine-induced spatial working memory deficits. *Peptides* **2010**, *31*, 2209–2215.
- (10) Olson, M. L.; Olson, E. A.; Qualls, J. H.; Stratton, J. J.; Harding, J. W.; Wright, J. W. Norleucine¹-angiotensin IV alleviates mecaminylamine-induced spatial memory deficits. *Peptides* **2004**, *25*, 233–241.
- (11) Tchekalarova, J.; Kambourova, T.; Georgiev, V. Interaction between angiotensin IV and adenosine A₁ receptor related drugs in passive avoidance conditioning in rats. *Behav. Brain Res.* **2001**, *123*, 113–116.
- (12) Wayner, M. J.; Armstrong, D. L.; Phelix, C. F.; Wright, J. W.; Harding, J. W. Angiotensin IV enhances LTP in rat dentate gyrus in vivo. *Peptides* **2001**, *22*, 1403–1414.
- (13) Wright, J. W.; Stuble, L.; Pederson, E. S.; Kramar, E. A.; Hanesworth, J. M.; Harding, J. W. Contributions of the brain angiotensin IV-AT₄ receptor subtype system to spatial learning. *J. Neurosci.* **1999**, *19*, 3952–3961.
- (14) Wright, J. W.; Clemens, J. A.; Panetta, J. A.; Smalstig, E. B.; Weatherly, L. A.; Kramar, E. A.; Pederson, E. S.; Mungall, B. H.; Harding, J. W. Effects of LY231617 and angiotensin IV on ischemia-induced deficits in circular water maze and passive avoidance performance in rats. *Brain Res.* **1996**, *717*, 1–11.
- (15) Wright, J. W.; Krebs, L. T.; Stobb, J. W.; Harding, J. W. The angiotensin IV system: functional implications. *Front. Neuroendocrinol.* **1995**, *16*, 23–52.
- (16) Wright, J. W.; Miller-Wing, A. V.; Shaffer, M. J.; Higginson, C.; Wright, D. E.; Hanesworth, J. M.; Harding, J. W. Angiotensin II(3-8) (ANG IV) hippocampal binding: potential role in the facilitation of memory. *Brain Res. Bull.* **1993**, *32*, 497–502.
- (17) Pederson, E. S.; Krishnan, R.; Harding, J. W.; Wright, J. W. A role for the angiotensin AT₄ receptor subtype in overcoming scopolamine-induced spatial memory deficits. *Regul. Pept.* **2001**, *102*, 147–156.
- (18) Pederson, E. S.; Harding, J. W.; Wright, J. W. Attenuation of scopolamine-induced spatial learning impairments by an angiotensin IV analog. *Regul. Pept.* **1998**, *74*, 97–103.
- (19) Wright, J. W.; Harding, J. W. The brain angiotensin IV/AT₄ receptor system as a new target for the treatment of Alzheimer's disease. *Drug Dev. Res.* **2009**, *70*, 472–480.
- (20) Albiston, A. L.; McDowall, S. G.; Matsacos, D.; Sim, P.; Clune, E.; Mustafa, T.; Lee, J.; Mendelsohn, F. A.; Simpson, R. J.; Connolly, L. M.; Chai, S. Y. Evidence that the angiotensin IV (AT₄) receptor is the enzyme insulin-regulated aminopeptidase. *J. Biol. Chem.* **2001**, *276*, 48623–48626.
- (21) Chai, S. Y.; Bastias, M. A.; Clune, E. F.; Matsacos, D. J.; Mustafa, T.; Lee, J. H.; McDowall, S. G.; Paxinos, G.; Mendelsohn, F. A.; Albiston, A. L. Distribution of angiotensin IV binding sites (AT₄ receptor) in the human forebrain, midbrain and pons as visualised by in vitro receptor autoradiography. *J. Chem. Neuroanat.* **2000**, *20*, 339–348.
- (22) Fernando, R. N.; Larm, J.; Albiston, A. L.; Chai, S. Y. Distribution and cellular localization of insulin-regulated aminopeptidase in the rat central nervous system. *J. Comp. Neurol.* **2005**, *487*, 372–390.
- (23) Moeller, I.; Paxinos, G.; Mendelsohn, F. A.; Aldred, G. P.; Casley, D.; Chai, S. Y. Distribution of AT₄ receptors in the *Macaca fascicularis* brain. *Brain Res.* **1996**, *712*, 307–324.
- (24) Keller, S. R.; Scott, H. M.; Mastick, C. C.; Aebersold, R.; Lienhard, G. E. Cloning and characterization of a novel insulin-regulated membrane aminopeptidase from Glut4 vesicles. *J. Biol. Chem.* **1995**, *270*, 23612–23618.
- (25) Olsen, J.; Cowell, G. M.; Konigshofer, E.; Danielsen, E. M.; Moller, J.; Laustsen, L.; Hansen, O. C.; Welinder, K. G.; Engberg, J.; Hunziker, W.; Complete amino acid sequence of human intestinal aminopeptidase N as deduced from cloned cDNA. *FEBS Lett.* **1988**, *238*, 307–314.
- (26) Chai, S. Y.; Yeatman, H. R.; Parker, M. W.; Ascher, D. B.; Thompson, P. E.; Mulvey, H. T.; Albiston, A. L. Development of cognitive enhancers based on inhibition of insulin-regulated aminopeptidase. *BMC Neurosci.* **2008**, *9* (Suppl. 2), S14.
- (27) Hallberg, M. Targeting the insulin-regulated aminopeptidase/AT₄ receptor for cognitive disorders. *Drug News Perspect.* **2009**, *22*, 133–139.
- (28) Wright, J. W.; Harding, J. W. The angiotensin AT₄ receptor subtype as a target for the treatment of memory dysfunction associated with Alzheimer's disease. *J. Renin—Angiotensin—Aldosterone Syst.* **2008**, *9*, 226–237.
- (29) Birks, J. Cholinesterase inhibitors for Alzheimer's disease. *Cochrane Database Syst. Rev.* **2006**No. CD005593.
- (30) Cosman, K. M.; Boyle, L. L.; Porsteinsson, A. P. Memantine in the treatment of mild-to-moderate Alzheimer's disease. *Expert Opin. Pharmacother.* **2007**, *8*, 203–214.
- (31) Doraiswamy, P. M.; Xiong, G. L. Pharmacological strategies for the prevention of Alzheimer's disease. *Expert Opin. Pharmacother.* **2006**, *7*, 1–10.
- (32) Raina, P.; Santaguida, P.; Ismaila, A.; Patterson, C.; Cowan, D.; Levine, M.; Booker, L.; Oremus, M. Effectiveness of cholinesterase inhibitors and memantine for treating dementia: evidence review for a clinical practice guideline. *Ann. Intern. Med.* **2008**, *148*, 379–397.
- (33) Krishnan, R.; Hanesworth, J. M.; Wright, J. W.; Harding, J. W. Structure–binding studies of the adrenal AT₄ receptor: analysis of position two- and three-modified angiotensin IV analogs. *Peptides* **1999**, *20*, 915–920.
- (34) Sardinia, M. F.; Hanesworth, J. M.; Krebs, L. T.; Harding, J. W. AT₄ receptor binding characteristics: D-amino acid- and glycine-substituted peptides. *Peptides* **1993**, *14*, 949–954.
- (35) Sardinia, M. F.; Hanesworth, J. M.; Krishnan, F.; Harding, J. W. AT₄ receptor structure–binding relationship: N-terminal-modified angiotensin IV analogues. *Peptides* **1994**, *15*, 1399–1406.
- (36) Wright, J. W.; Harding, J. W. The brain RAS and Alzheimer's disease. *Exp. Neurol.* **2010**, *223*, 326–333.
- (37) McCoy, A. Pharmacokinetic Characterization of Angiotensin IV Analogs with Therapeutic Potential for Cancer and Dementia. Ph.D. Thesis, Washington State University, Washington, DC, 2010.
- (38) Lukaszuk, A.; Demaegd, H.; Feytens, D.; Vanderheyden, P.; Vauquelin, G.; Tourwe, D. The replacement of His⁴ in angiotensin IV by conformationally constrained residues provides highly potent and selective analogues. *J. Med. Chem.* **2009**, *52*, 5612–5618.
- (39) Lukaszuk, A.; Demaegd, H.; Szemenyei, E.; Toth, G.; Ty-mecka, D.; Misicka, A.; Karoyan, P.; Vanderheyden, P.; Vauquelin, G.; Tourwe, D. β-Homo-amino acid scan of angiotensin IV. *J. Med. Chem.* **2008**, *51*, 2291–2296.
- (40) Albiston, A. L.; Morton, C. J.; Ng, H. L.; Pham, V.; Yeatman, H. R.; Ye, S.; Fernando, R. N.; De Bundel, D.; Ascher, D. B.; Mendelsohn, F. A.; Parker, M. W.; Chai, S. Y. Identification and characterization of a new cognitive enhancer based on inhibition of insulin-regulated aminopeptidase. *FASEB J.* **2008**, *22*, 4209–4217.
- (41) Albiston, A. L.; Pham, V.; Ye, S.; Ng, L.; Lew, R. A.; Thompson, P. E.; Holien, J. K.; Morton, C. J.; Parker, M. W.; Chai, S. Y. Phenylalanine-544 plays a key role in substrate and inhibitor binding by providing a hydrophobic packing point at the active site of insulin-regulated aminopeptidase. *Mol. Pharmacol.* **2010**, *78*, 600–607.
- (42) Andersson, H.; Demaegd, H.; Vauquelin, G.; Lindeberg, G.; Karlen, A.; Hallberg, M. Ligands to the (IRAP)/AT₄ receptor encompassing a 4-hydroxydiphenylmethane scaffold replacing Tyr². *Bioorg. Med. Chem.* **2008**, *16*, 6924–6935.
- (43) Axén, A.; Andersson, H.; Lindeberg, G.; Ronnholm, H.; Kortessmaa, J.; Demaegd, H.; Vauquelin, G.; Karlen, A.; Hallberg, M.

Small potent ligands to the insulin-regulated aminopeptidase (IRAP)/AT₄ receptor. *J. Pept. Sci.* **2007**, *13*, 434–444.

(44) Axén, A.; Lindeberg, G.; Demaegd, H.; Vauquelin, G.; Karlén, A.; Hallberg, M. Cyclic insulin-regulated aminopeptidase (IRAP)/AT₄ receptor ligands. *J. Pept. Sci.* **2006**, *12*, 705–713.

(45) Andersson, H.; Demaegd, H.; Vauquelin, G.; Lindeberg, G.; Karlen, A.; Hallberg, M.; Erdelyi, M.; Hallberg, A. Disulfide cyclized tripeptide analogues of angiotensin IV as potent and selective inhibitors of insulin-regulated aminopeptidase (IRAP). *J. Med. Chem.* **2010**, *53*, 8059–8071.

(46) Driggers, E. M.; Hale, S. P.; Lee, J.; Terrett, N. K. The exploration of macrocycles for drug discovery—an underexploited structural class. *Nat. Rev. Drug Discovery* **2008**, *7*, 608–624.

(47) Fu, G. C.; Grubbs, R. H. The application of catalytic ring-closing olefin metathesis to the synthesis of unsaturated oxygen heterocycles. *J. Am. Chem. Soc.* **1992**, *114*, 5426–5427.

(48) Fu, G. C.; Nguyen, S. T.; Grubbs, R. H. Catalytic ring-closing metathesis of functionalized dienes by a ruthenium carbene complex. *J. Am. Chem. Soc.* **1993**, *115*, 9856–9857.

(49) Jiang, S.; Li, Z.; Ding, K.; Roller, P. P. Recent progress of synthetic studies to peptide and peptidomimetic cyclization. *Curr. Org. Chem.* **2008**, *12*, 1502–1542.

(50) Miller, S. J.; Blackwell, H. E.; Grubbs, R. H. Application of ring-closing metathesis to the synthesis of rigidified amino acids and peptides. *J. Am. Chem. Soc.* **1996**, *118*, 9606–9614.

(51) Miller, S. J.; Grubbs, R. H. Synthesis of conformationally restricted amino acids and peptides employing olefin metathesis. *J. Am. Chem. Soc.* **1995**, *117*, 5855–5856.

(52) Berezowska, I.; Chung, N. N.; Lemieux, C.; Wilkes, B. C.; Schiller, P. W. Cyclic dermorphin tetrapeptide analogues obtained via ring-closing metathesis. *Acta Biochim. Pol.* **2006**, *53*, 73–76.

(53) Berezowska, I.; Chung, N. N.; Lemieux, C.; Wilkes, B. C.; Schiller, P. W. Dicarba analogues of the cyclic enkephalin peptides H-Tyr-c[D-Cys-Gly-Phe-D(or L)-Cys]NH₂ retain high opioid activity. *J. Med. Chem.* **2007**, *50*, 1414–1417.

(54) D'Addona, D.; Carotenuto, A.; Novellino, E.; Piccand, V.; Reubi, J. C.; Di Cianni, A.; Gori, F.; Papini, A. M.; Ginanneschi, M. Novel sst₅-selective somatostatin dicarba-analogues: synthesis and conformation–affinity relationships. *J. Med. Chem.* **2008**, *51*, 512–520.

(55) Fang, W. J.; Cui, Y.; Murray, T. F.; Aldrich, J. V. Design, synthesis, and pharmacological activities of dynorphin A analogues cyclized by ring-closing metathesis. *J. Med. Chem.* **2009**, *52*, 5619–5625.

(56) Stymiest, J. L.; Mitchell, B. F.; Wong, S.; Vederas, J. C. Synthesis of oxytocin analogues with replacement of sulfur by carbon gives potent antagonists with increased stability. *J. Org. Chem.* **2005**, *70*, 7799–7809.

(57) Carpino, L. A.; Han, G. Y. 9-Fluorenylmethoxycarbonyl amino-protecting group. *J. Org. Chem.* **1972**, *37*, 3404–3409.

(58) Chapman, R. N.; Arora, P. S. Optimized synthesis of hydrogen-bond surrogate helices: surprising effects of microwave heating on the activity of Grubbs catalysts. *Org. Lett.* **2006**, *8*, 5825–5828.

(59) *Stability of Polymer-Supports to Microwave Heating*; Novabiochem Innovations 4/03; EMD Biosciences Inc.: La Jolla, CA.

(60) Ahn, Y. M.; Yang, K.; Georg, G. I. A convenient method for the efficient removal of ruthenium byproducts generated during olefin metathesis reactions. *Org. Lett.* **2001**, *3*, 1411–1413.

(61) Stymiest, J. L.; Mitchell, B. F.; Wong, S.; Vederas, J. C. Synthesis of biologically active dicarba analogues of the peptide hormone oxytocin using ring-closing metathesis. *Org. Lett.* **2003**, *5*, 47–49.

(62) Hong, S. H.; Sanders, D. P.; Lee, C. W.; Grubbs, R. H. Prevention of undesirable isomerization during olefin metathesis. *J. Am. Chem. Soc.* **2005**, *127*, 17160–17161.

(63) Kay, C.; Lorthioir, O. E.; Parr, N. J.; Congreve, M.; McKeown, S. C.; Scicinski, J. J.; Ley, S. V. Solid-phase reaction monitoring—chemical derivatization and off-bead analysis. *Biotechnol. Bioeng.* **2000**, *71*, 110–118.

(64) Vojtkovsky, T. Detection of secondary amines on solid phase. *Pept. Res.* **1995**, *8*, 236–237.

(65) Tang, Z. L.; Pelletier, J. C. Preparation of amides from acids and resin bound azides: suppression of intramolecular lactam formation. *Tetrahedron Lett.* **1998**, *39*, 4773–4776.

(66) Brandt, M.; Gammeltoft, S.; Jensen, K. Microwave heating for solid-phase peptide synthesis: general evaluation and application to 15-mer phosphopeptides. *Int. J. Pept. Res. Ther.* **2006**, *12*, 349–357.

(67) Vázquez, J.; Albericio, F. A useful and sensitive color test to monitor aldehydes on solid-phase. *Tetrahedron Lett.* **2001**, *42*, 6691–6693.

(68) Sheppeck, J. E.; Kar, H.; Hong, H. A convenient and scaleable procedure for removing the Fmoc group in solution. *Tetrahedron Lett.* **2000**, *41*, 5329–5333.

(69) Griesinger, C.; Sørensen, O. W.; Ernst, R. R. Practical aspects of the E.COSY technique. Measurement of scalar spin–spin coupling constants in peptides. *J. Magn. Reson.* **1987**, *75*, 474–492.

(70) Kumar, A.; Ernst, R. R.; Wüthrich, K. A two-dimensional nuclear Overhauser enhancement (2D NOE) experiment for the elucidation of complete proton–proton cross-relaxation networks in biological macromolecules. *Biochem. Biophys. Res. Commun.* **1980**, *95*, 1–6.

(71) Mueller, L. P. E. COSY, a simple alternative to E.COSY. *J. Magn. Reson.* **1987**, *72*, 191–196.

(72) Demaegd, H.; Laeremans, H.; De Backer, J.-P.; Mosselmans, S.; Le, M. T.; Kersemans, V.; Michotte, Y.; Vauquelin, G.; Vanderheyden, P. M. L. Synergistic modulation of cystinyl aminopeptidase by divalent cation chelators. *Biochem. Pharmacol.* **2004**, *68*, 893–900.

(73) Demaegd, H.; Lenaerts, P. J.; Swales, J.; De Backer, J. P.; Laeremans, H.; Le, M. T.; Kersemans, K.; Vogel, L. K.; Michotte, Y.; Vanderheyden, P.; Vauquelin, G. Angiotensin AT₄ receptor ligand interaction with cystinyl aminopeptidase and aminopeptidase N: [¹²⁵I]angiotensin IV only binds to the cystinyl aminopeptidase apoenzyme. *Eur. J. Pharmacol.* **2006**, *546*, 19–27.

(74) Laeremans, H.; Demaegd, H.; De Backer, J. P.; Le, M. T.; Kersemans, V.; Michotte, Y.; Vauquelin, G.; Vanderheyden, P. M. Metal ion modulation of cystinyl aminopeptidase. *Biochem. J.* **2005**, *390*, 351–357.

(75) Vanderheyden, P. M.; Demaegd, H.; Swales, J.; Lenaerts, P. J.; De Backer, J. P.; Vogel, L. K.; Vauquelin, G. Synergistic inhibition of the enzymatic activity of aminopeptidase N by divalent metal ion chelators. *Fundam. Clin. Pharmacol.* **2006**, *20*, 613–619.

(76) Demaegd, H.; Lukaszuk, A.; De Buysers, E.; De Backer, J. P.; Szemenyei, E.; Toth, G.; Chakravarthy, S.; Panicker, M.; Michotte, Y.; Tourwe, D.; Vauquelin, G. Selective labeling of IRAP by the tritiated AT₄ receptor ligand [³H]angiotensin IV and its stable analog [³H]AL-11. *Mol. Cell. Endocrinol.* **2009**, *311*, 77–86.

(77) Grauer, A.; König, B. Peptidomimetics—a versatile route to biologically active compounds. *Eur. J. Org. Chem.* **2009**, *2009*, 5099–5111.

(78) Mollica, A.; Paglialonga Paradisi, M.; Torino, D.; Spisani, S.; Lucente, G. Hybrid α/β -peptides: for-Met-Leu-Phe-OME analogues containing geminally disubstituted $\beta^{2,2}$ - and $\beta^{3,3}$ -amino acids at the central position. *Amino Acids* **2006**, *30*, 453–459.

(79) Schumann, F.; Müller, A.; Kokschi, M.; Müller, G.; Sewald, N. Are β -amino acids γ -turn mimetics? Exploring a new design principle for bioactive cyclopeptides. *J. Am. Chem. Soc.* **2000**, *122*, 12009–12010.

(80) Aguilar, M. I.; Purcell, A. W.; Devi, R.; Lew, R.; Rossjohn, J.; Smith, A. I.; Perlmutter, P. Beta-amino acid-containing hybrid peptides—new opportunities in peptidomimetics. *Org. Biomol. Chem.* **2007**, *5*, 2884–2890.

(81) Chatterjee, J.; Gilon, C.; Hoffman, A.; Kessler, H. N-Methylation of peptides: a new perspective in medicinal chemistry. *Acc. Chem. Res.* **2008**, *41*, 1331–1342.

(82) Rajeswaran, W. G.; Hocart, S. J.; Murphy, W. A.; Taylor, J. E.; Coy, D. H. N-Methyl scan of somatostatin octapeptide agonists produces interesting effects on receptor subtype specificity. *J. Med. Chem.* **2001**, *44*, 1416–1421.

(83) Kiyoshi, I.; Yoshitaka, N.; Yuko, O.; Masahide, T.; Kanako, N.; Futoshi, M.; Takashi, I.; Tadashi, Y. Crystal structure of aminopeptidase N (proteobacteria alanyl aminopeptidase) from *Escherichia coli* and conformational change of methionine 260 involved in substrate recognition. *J. Biol. Chem.* **2006**, *281*, 33664–33676.

(84) Tholander, F.; Muroya, A.; Roques, B. P.; Fournie-Zaluski, M. C.; Thunnissen, M. M.; Haeggstrom, J. Z. Structure-based dissection of the active site chemistry of leukotriene A4 hydrolase: implications for M1 aminopeptidases and inhibitor design. *Chem. Biol.* **2008**, *15*, 920–929.

(85) Ye, S.; Chai, S. Y.; Lew, R. A.; Ascher, D. B.; Morton, C. J.; Parker, M. W.; Albiston, A. L. Identification of modulating residues defining the catalytic cleft of insulin-regulated aminopeptidase. *Biochem. Cell Biol.* **2008**, *86*, 251–261.

(86) Sigel, H.; Martin, R. B. Coordinating properties of the amide bond. Stability and structure of metal ion complexes of peptides and related ligands. *Chem. Rev.* **1982**, *82*, 385–426.

(87) Stadler, A.; Kappe, C. O. The effect of microwave irradiation on carbodiimide-mediated esterifications on solid support. *Tetrahedron* **2001**, *57*, 3915–3920.

(88) Johansen, T. E.; Scholler, M. S.; Tolstoy, S.; Schwartz, T. W. Biosynthesis of peptide precursors and protease inhibitors using new constitutive and inducible eukaryotic expression vectors. *FEBS Lett.* **1990**, *267*, 289–294.

(89) Le, M. T.; De Backer, J. P.; Hunyady, L.; Vanderheyden, P. M.; Vauquelin, G. Ligand binding and functional properties of human angiotensin AT₁ receptors in transiently and stably expressed CHO-K1 cells. *Eur. J. Pharmacol.* **2005**, *513*, 35–45.

(90) Demaegdt, H.; Vanderheyden, P.; De Backer, J. P.; Mosselmans, S.; Laeremans, H.; Le, M. T.; Kersemans, V.; Michotte, Y.; Vauquelin, G. Endogenous cystinyl aminopeptidase in Chinese hamster ovary cells: characterization by [¹²⁵I]Ang IV binding and catalytic activity. *Biochem. Pharmacol.* **2004**, *68*, 885–892.

(91) Cheng, Y.; Prusoff, W. H. Relationship between the inhibition constant (K_i) and the concentration of inhibitor which causes 50 per cent inhibition (IC_{50}) of an enzymatic reaction. *Biochem. Pharmacol.* **1973**, *22*, 3099–3108.